Special Issue: Unmanned Marine Systems

Regular Article

Ad hoc Acoustic Network Aided Localization for micro-AUVs

Davide Fenucci[1], Jeremy Sitbon[2], Jeffrey Neasham[3], Alexander B. Phillips[1] and Andrea Munafò[4]

[1]Marine Autonomous and Robotic Systems, National Oceanography Centre, Southampton, SO14 3ZH, UK
[2]ecoSub Robotics ltd., Southampton, SO14 3ZH, UK
[3]School of Engineering, Newcastle University, Newcastle upon Tyne, NE1 7RU, UK
[4]University of Pisa, Department of Information Engineering, Pisa, Italy

Abstract: The navigation of Autonomous Underwater Vehicles (AUVs) is still an open research problem. This is further exacerbated when vehicles can only carry limited sensors as typically the case with micro-AUVs that need to survey large marine areas that can be characterized by high currents and dynamic environments. To address this problem, this work investigates the usage of *ad hoc* acoustic networks that can be established by a set of cooperating vehicles. Leveraging the network structure makes it possible to greatly improve the navigation of the vehicles and as a result to enlarge the operational envelope of vehicles with limited capabilities. The paper details the design and implementation of the network, and specific details of localization and navigation services made available to the vehicles by the network stack. Results are provided from a sea-trial undertaken in Croatia in October 2019. Results validate the approach, demonstrating the increased flexibility of the system and the navigational performance obtained: the deployed network was able to support long-range navigation of vehicles with no inertial navigation or Doppler Velocity Log (DVL) during a 9.5 km channel crossing, reducing the navigation error from approximately 7% to 0.27% of the distance traveled.

Keywords: underwater robotics, sensor networks, cooperative robots, localization, navigation

1. Introduction

The achieved maturity of Autonomous Underwater Vehicle (AUV) and communication technologies (Song et al., 2019) is paving the way to simultaneous deployment of multiple vehicles that can be intelligently interconnected to achieve a network multiplier that is able to overcome the limitations of the individual platforms. The potential benefits of utilising fleets of AUVs have been well documented (Jones et al., 2019). Today, multiple AUVs are deployed to obtain multiple parallel measurements providing a synoptic picture of the environment and increased level of mission robustness and redundancy. Recent examples include the deployment of swarms of miniautonomous underwater

Received: 21 September 2021; revised: 29 June 2022; accepted: 9 August 2022; published: 19 September 2022.

Correspondence: Davide Fenucci, Marine Autonomous and Robotic Systems, National Oceanography Centre, Southampton, SO14 3ZH, UK, Email: davfen@noc.ac.uk

DOI: https://doi.org/10.55417/fr.2022059

explorers able to independently measure changes of the nonlinear dynamics of the ocean, sampling simultaneously at multiple locations (Jaffe et al., 2017). The benefit of deploying networked AUVs to environmental assess and monitor decommissioned oil and gas field is reported in (Jones et al., 2019), where the ability to leverage multisensor views to monitor these challenging sites can lead to cost savings and to a substantial improvement in the temporal and spatial resolution of the observations. In defence scenarios, collaborative multivehicle missions are routinely demonstrated where the autonomy installed on multiple vehicles work together to intelligently execute tasks (SeeByte, ltd., 2021; Ferri et al., 2020). While these deployments are a reality, the size of the fleet is still, in the majority of cases, composed only of a few vehicles, mostly limited by the logistical difficulty of operations and by the costs involved with larger deployments. Larger networks however are becoming increasingly feasible with the emerging class of low-cost, low-power micro-AUVs (Schill et al., 2018; Fenucci et al., 2018). These smaller vehicles can typically only carry limited payloads due to the limited space, energy and compute power available, and when used in isolation this can substantially limit their operational envelope. However, when deployed in a network, they can share information and have access to additional services that can alleviate some of their limitations and even achieve performance levels that would not be possible otherwise. This paper tackles this specific aspect, and it aims at showing how the ability of micro-AUVs to exploit network-level services makes it possible to substantially increase their navigation performance.

1.1. Related work

The attenuation of radio-frequency signals coupled with dynamic and unstructured environments makes underwater navigation and localization a challenging task. Once submerged AUVs are no longer able to resort to Global Navigation Satellite Systems (GNSS) such as the Global Positioning System (GPS) and typically rely on dead reckoning, i.e., integration of speed and heading with respect to time. The accuracy of the approach is highly dependent on the sensors fitted to the vehicle. For high power AUVs, the usage of a DVL coupled with an Inertial Navigation System (INS) can achieve navigational errors of ∼0.1% of the distance traveled in a straight line. Using a DVL, however, requires higher power and constrains AUVs to operate within a few hundred metres from the seabed to have a consistent lock on the bottom. For open water operations where vehicles are required to move through the water column or far from the bottom, DVLs can only be used for water velocity measurements that cannot be used to limit navigational errors associated with movements of the water. For micro-AUVs operating in such scenarios, the typical alternative is to integrate simplified velocity models (e.g., speed estimate from the propeller rotational speed) with the orientation provided from a low-cost Inertial Measurement Unit (IMU). Navigation errors for these set-ups are as high as 20% of the distance traveled relative to the water (Munafò and Ferri, 2017). Alternatively, to compensate for the unavoidable drift, missions can be set up to command the vehicles to perform frequent surfacing and obtain GPS fixes. Note that this approach, which is quite often used in practise, leads to task interruptions and puts the vehicle at increased risk whilst on the surface. Moreover, when vehicles are working in very deep water, the cost associated with requiring a vehicle to repeatedly surface can be significant in terms of both time and energy expenditure. In such situations, the benefits of surfacing may also be limited, as the drift errors are unconstrained while the vehicle is transiting across the mid-water column, and unable to measure movement due to currents in relation to the seafloor. One effective way of bounding the navigation error can be achieved using external acoustic aiding. Long Base Line (LBL) systems combine range measurements from static acoustic nodes with an on-board navigation filter to derive a position estimate. Ultra-Short Base Line (USBL) systems couple a transceiver composed of an array of transducers to determine range and angle to a pairing device. USBL devices are typically mounted on a ship or on a Unmanned Surface Vehicle (USV) that acts as a navigation aid for the underwater robot (Phillips et al., 2018). The use of static or dedicated beacons avoids the problem of cumulative drift, but imposes constraints on the operational area, reducing the freedom of movement of the vehicles. Depending on the scenario, this might be incompatible with the higher-level mission requirements

(e.g., when operating on large scales, such as inspecting a pipeline, or when the topology of the feature of interest is dynamic or unknown in advance, such as when mapping a hydrocarbon plume). Moreover, to obtain a good navigational fix, multiple dedicated beacons must be deployed to achieve the necessary spatial diversity. Deploying beacons, and navigating them in to provide a known location, requires a great deal of instrumentation to be deployed and calibrated at each site. This is time consuming and impracticable for many operational scenarios.

The use of a network of cooperating vehicles to support navigation has been recently suggested as an effective alternative to improve the navigation of underwater vehicles. The presence of networked communications opens up the possibility to acquire intervehicle relative positioning data and to use them to aid vehicle navigation. Depending on the equipment installed on-board, each vehicle/node in the network can have access to different sources of relative positioning measures: the distance, or range, from another vehicle calculated using the time of flight (TOF) of a transmitted signal (two-way, or one-way in case of synchronized clocks); the relative direction, or bearing, obtained from the difference in the phases of a signal received by each transducer of an acoustic array; or a combination of both if a USBL is available. This type of information could provided as a built-in functionality of the acoustic devices in use, or it might be developed as an additional layer built on top of the capabilities provided at the physical layer. For instance, (Munafò and Ferri, 2017) implemented an opportunistic ranging algorithm that relies on an interrogation scheme similar to that of a LBL but managed at the network level. The exploitation of message transmission and reception times at the network application layer makes it possible to add localization services to the underlying underwater network, increasing the system flexibility. For example, new nodes can be added or removed as they join or leave the network without the need for explicit re-configurations. Another example is described in (Quraishi et al., 2019), where the system uses absolute time information from GNSS for initial clock synchronization and relies on one-way travel time (OWTT) for determining range measurements. The system does not rely on any installed infrastructure in the environment, and the use of synchronized clocks makes it scalable in the number of robots. The system operation time depends on the stability of the clocks and might require periodic re-synchronization to avoid ranging errors (Vermeij and Munafò, 2015). Moreover, the association between a range measurements and the corresponding transmission node, requires the shared knowledge of the transmission schedule before the mission, hence making it difficult to dynamically adapt the network when operational requirements change.

Another important aspect to consider in networked systems is represented by the management of the access to the shared communication medium, i.e., the acoustic channel. In typical configurations for underwater sensor networks, the physical layer does not specify any Medium Access Control (MAC) to handle collisions, and packet scheduling is managed at a higher level according to a well defined network policy. The choice of a MAC is important not only in terms of packet delivery and network throughput, but also because it can have a direct impact on how many localization messages are received by each node, and hence on its navigational performance (Śliwka et al., 2017). More information on available MAC protocols for underwater networks are reported in (Jiang, 2018; Petrioli et al., 2008) and references therein.

The relative positioning methods described above can be integrated in a cooperative underwater navigation framework using two different approaches. A first approach is to specialize some of the team members, called Communication and Navigation Aids (CNAs), providing them with enhanced navigation capabilities (e.g., high-precision INS, constant or frequent access to GPS, etc.). CNAs employ acoustic modems to periodically transmit an estimate of their position through the acoustic network. The remaining vehicles can then combine these information with relative positioning measurements with respect to the CNAs acquired on-board to self-localize and bound the error of the dead-reckoning navigation. This concept, referred to as *heterogeneous AUV team* (Paull et al., 2014a), is explored, among others, in (Quraishi et al., 2019; Munafò and Ferri, 2017; Bahr et al., 2009a). Despite subtracting some vehicle(s) from accomplishing mission-related tasks, this scheme scales relatively well, as it has limited communication requirements: the usage of the acoustic network is in fact restricted to the transmission of instantaneous CNAs position estimates and the acquisition

of relative positioning data. In the second approach, all the team members are considered to have the same capabilities and it is hence referred to as *homogeneous AUV team* (Paull et al., 2014a). Each vehicle exploits relative position measurements from any of the other nodes, integrating them in a distributed cooperative navigation algorithm that estimates the full navigation state of the team. To ensure the position estimate remains consistent over time, cross-covariance terms must be carefully accounted for (Roumeliotis and Bekey, 2002), requiring an increased communication load to transmit all the data needed. This scheme allows the whole team to effectively participate in mission operations, but it might require a high load on the network (Li et al., 2019; Paull et al., 2014b), or slightly degraded navigation performance over time (Maczka et al., 2007; Bahr et al., 2009b). In this case, a trade-off between navigation accuracy and communication overhead must then be established, and potential re-transmissions due to packet losses should be carefully addressed (Fallon et al., 2010).

The choice between setting up a heterogeneous or a homogeneous team, the relative positioning measurement to use, and whether or not to implement a MAC for the network depends on the application and operational environment, and typically there is not a "one size fits all" solution for every scenario, or even for a single scenario. Environmental changes might drive vehicles out of the expected communication range, or vehicle failures might compromise some of the assigned anchor points and hence lead to different navigational choices.

1.2. Contribution of this work

This paper builds on these recent results and describes a layered, service-oriented architecture designed to accommodate the needs of *ad hoc* acoustic sensor networks of micro-AUVs in different application scenarios, with the aim of providing the necessary services and infrastructure to enable the operation of a fleet of small, low-cost underwater vehicles. Initial concepts about the benefits of having an interplay between the autonomy and the communication systems of an AUV have been proposed by the authors in (Hamilton et al., 2020), together with an initial experimental assessment of the implemented network. Building on those early concepts, the contribution of this work is twofold.

(1) It presents the design of a networked architecture composed of cross-functional layers to support the navigation, localization and autonomy of AUVs. Moving most of the communication processing from the physical level to the network level makes it possible to abstract the network design away from the specific hardware requirements. Such a design is particularly attractive for inexpensive vehicles, heterogeneous fleets and in scenarios where there is the need to limit costs. The paper discusses how making communications and localization data available as a network service simplifies the design of the AUVs on-board control system, increasing the system flexibility and ultimately mission performance: every node able to communicate with the network can also obtain the additional advantages of being part of a structured ecosystem and hence have access to the entire list of services provided.

(2) It provides a concrete implementation of the proposed architecture for an *ad hoc* network of micro-AUVs operating in harsh, high current and tidal environments, with the aim of experimentally demonstrating the benefits of the proposed cooperative navigation system over traditional dead-reckoning based solutions for low-cost, low-energy vehicles. Experimental results are reported from sea-trials undertaken in Biograd Na Moru, Croatia in September 2019 where a network of up to six AUVs was deployed. Results demonstrate how the network is able to robustly adjust as the number of vehicles is increased, the availability of navigational aids vary, and how the system is effective at supporting long-range navigation of a vehicle with no inertial navigation and DVL during a 9.5 km channel crossing, reducing the navigation error from approximately 7% to 0.27% of the distance traveled.

The paper reports and discusses the entire network stack as an adaptive and cross-functional layering for navigation, localization, autonomy and communications. However, only the navigation, localization and communications services have been evaluated and tested during the reported experiments. It is the authors' belief that reporting field performance, even when it is for a subset of

the implemented features is of value in itself. It can be useful to practitioners interested in specific applications and can orient research towards refinements or towards different choices.

The remainder of this paper is organized as follows. Section 2 sets up the problem, and discusses the system design. Section 3 describes the experimental set-up that was deployed to verify and validate the system. Section 4 details the obtained experimental results, while Section 5 discusses the main lessons learnt. Finally, Section 6 draws conclusions and points out some future research lines.

2. System overview

This work tackles the problem of surveying large marine areas using a swarm of micro-AUVs. There are no assumptions on the operational environment, which in general is dynamic and may be characterized by high currents and tides. Micro-AUVs are typically limited in their payload capacity, and often used in applications where reducing costs is important and this further constraints the ability of using high performance sensors. Key to this concept is the availability of reliable movable nodes that can flexibly adapt to changing environmental or mission conditions, and of vehicle-to-vehicle interconnections to share information across the fleet to enable a network gain that can overcome the limitation of the individual platforms. For example, vehicles with limited navigation capacity can take advantage from the network to improve their localization. At the same time, to increase the system flexibility, each node is designed to be fully self-contained, or, in other words, able to work independently when needed (e.g., no communication is available), autonomously reacting to change in the environment or in the mission requirements.

This section describes the proposed service-oriented architecture to enable networked localization capabilities and cooperative behaviors among the team of vehicles. To demonstrate the effectiveness of the approach, the presented concepts have been developed and implemented for a network of micro-AUVs that it is used as representative case study. In the considered application, the fleet is assumed to be composed of heterogeneous vehicles: part of the AUVs are set up as surface nodes receiving GNSS position updates and acting as reference beacons for submerged nodes. The other vehicles act as submerged nodes receiving range information from the surface ones and using them to improve their localization. The division between surface or underwater nodes is initially determined before the deployment, but for the requirements of the considered application, it must be possible to be dynamically adapted: a surface vehicle can become an underwater node and vice versa. All the vehicles in the team run an instance of the developed modules for networked acoustic communication, localization data gathering and estimation of the navigation state. This makes it possible for each vehicle to opportunistically leverage the presence of collaborators that might be in their vicinity to improve their navigation, or to act as navigation aid for other nodes. The developed *ad hoc* network is illustrated in Figure 1.

2.1. Acoustic network

The acoustic network represents the backbone of the envisaged system, being the enabler for the inter-vehicle communication and for the vehicle cooperation. This section describes the selection and the development of network protocols and algorithms, the definition of messages and network services able to support multivehicle localization while minimising the communication overhead that is required to support the network. The network was developed according to the Software Defined Open Architecture Modems paradigm (Dol et al., 2017) to make it applicable to a range of communication devices. Within this concept, the acoustic network is responsible for encoding and decoding the relevant information as necessary, and it is able to adapt to the available acoustic modems. For example, to support localization, the network can measure the two-way travel time (TWTT) between transponders, and convert it into distances using measured or estimated sound speed values, or it can exploit the availability of synchronized clocks to reduce the number of messages required using OWTT. The *ad hoc* network is designed to explicitly use a set of potentially movable and cooperating nodes, and to accommodate for complex decision making that can happen

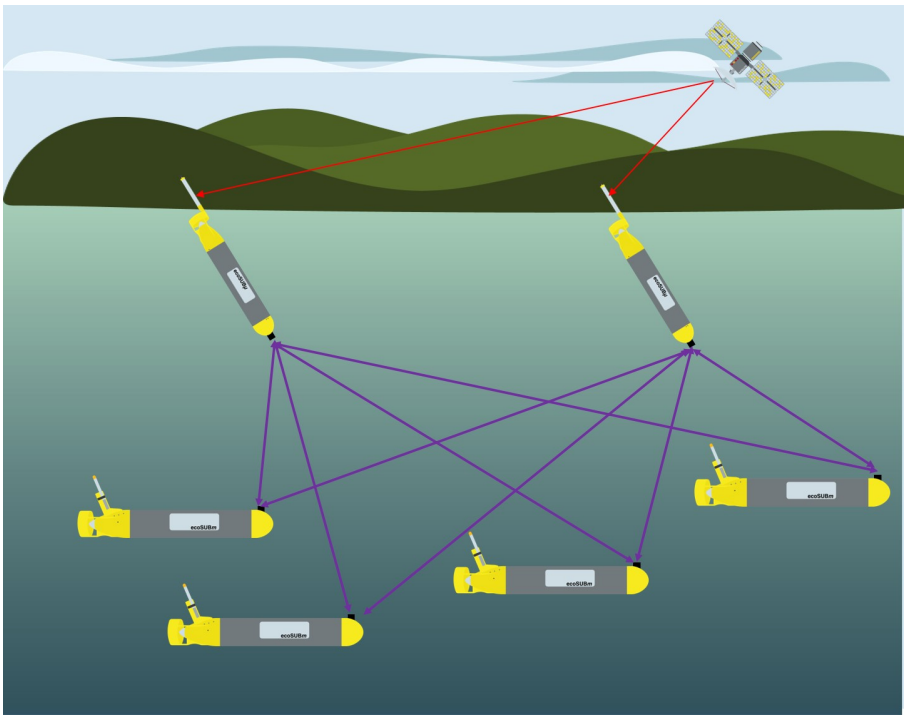

Figure 1. *Ad hoc* fleet concept, when deployed in the fleet the AUVs can act as surface nodes receiving GNSS position updates and providing reference beacons for submerged nodes or act as submerged nodes receiving range information from the surface nodes.

at application level to support navigation and localization. The existing communication and network infrastructure can be exploited to provide navigational services without the need to deploy dedicated transponders, and the nodes/AUVs are able to autonomously adapt the geometric configuration of the network, for example, selecting which subset of the nodes should move to the surface to provide global localization. The system is based on a Service-Oriented Network Architecture (SONA) to simplify sharing of information both at network level and at the autonomy level, and more broadly across the system. The network stack designed to support the multivehicle system is depicted in Figure 2. It provides two main services, communications and localization, which are described in the remainder of the section.

2.1.1. Communication service

The communication service enables the transmission and the reception of data through the acoustic channel. It was developed through the typical structure of an underwater acoustic network, from the physical layer up to the application layer. As typically done in underwater networks, there is no strict layer separation, but rather each element of the network is implemented as a module that can easily access relevant information as needed across the full stack.

Physical layer: miniature acoustic modems

Figure 3 shows the miniature, low-cost, low-power acoustic modems developed at Newcastle University (Lowes et al., 2019) (Neasham et al., 2015), which were used in these experiments. They measure only 42 mm diameter by 60 mm long when the transducer and the electronic circuit are encapsulated together, but a shorter moulded transducer assembly is mounted on the nose of the vehicle with the circuit mounted inside the main pressure housing. Operating in the acoustic frequency band 24–32 kHz, the latest generation of these modems (v3) employ spread spectrum modulation based on a variant of M-ary Orthogonal Signalling using pseudorandom Phase Shift

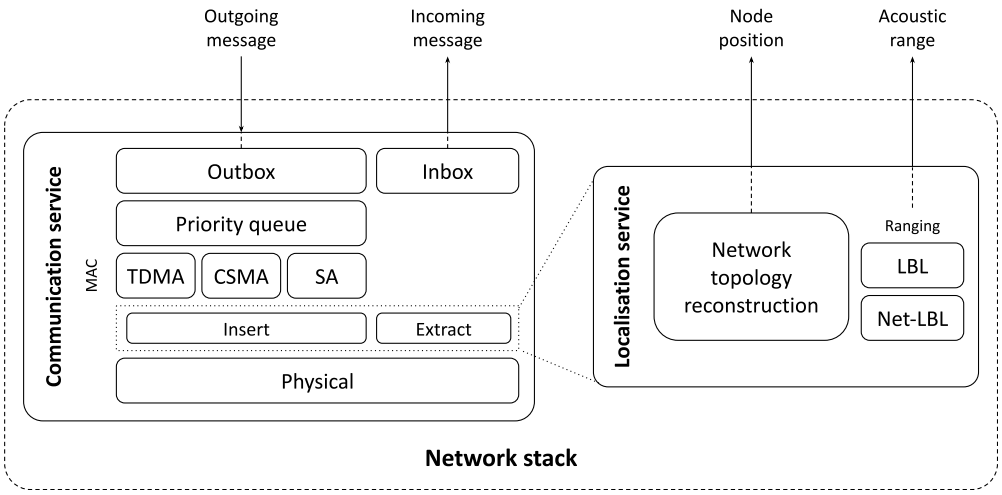

Figure 2. Conceptual block diagram of the network stack developed for the multivehicle system.

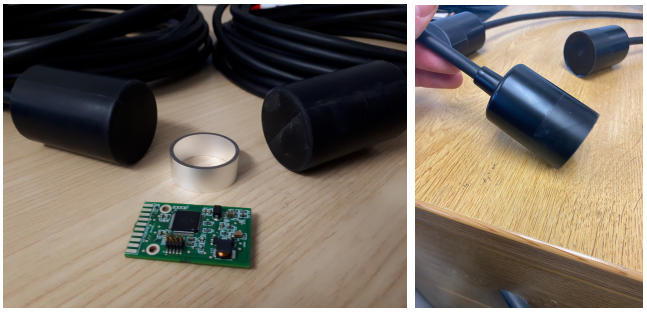

Figure 3. Miniature acoustic modems developed by Newcastle University (Sherlock et al., 2022).

Keyed (PSK) waveforms. This achieves a raw data rate of 640 bps over ranges up to 2 km. Net data throughput, taking into account packet framing and error correction overheads is up to 460 bps with data packets up to 64 B. This is achieved with a relatively low transmitted source power level of 168 dB re 1 uPa @ 1 m (∼0.5 W), while a highly efficient receiver implementation leads to power consumption of only 12.5 mW while listening and 25 mW when receiving a message. Range between devices can also be measured to a resolution of 5 cm, assuming a sound speed of 1500 m/s.

The modem hardware interfaces to a PC or other processor platform via RS232 at 9600 baud rate. Implementation of a robust spread spectrum receiver with minimal energy and processor cost has been enabled by several innovations in sparse signal processing to reduce the computational load whilst maintaining high processing gain and immunity to the severe multipath distortions commonly found in the underwater channel.

The modem is able to send messages with four transmission modalities.

- Unicasts (U): messages that are sent to a specific receiver.
- Broadcasts (B): messages that can be sent to all of receivers in the network at once.
- Unicasts with acknowledgement (M): messages that are sent to a specific destination host. The receiver must reply with a fixed, known turnaround time. When this modality is used, the transmitter automatically calculates the range to the receiver using the measured two-way-travel-time.
- Pings (P): these are two bytes messages that can be sent to verify if a receiving modem is alive, in communication range and/or to obtain a range measurement. A ping message is the shortest possible unicast message with acknowledgment.

These devices were developed as part of the EPSRC USMART project (Newcastle University and Heriott Watt and University of York, 2021) to provide a communication and positioning building block for large scale, cost effective wireless sensor networks to be constructed subsea. The unique low-cost, low-power and small dimensions of these modems made them the ideal technology for integration with micro-AUVs.

Data-link layer

The data-link layer implements the MAC policy, responsible for sharing the acoustic channel across the network nodes. While the network itself is independent of the specific MAC, its choice and configuration influences the quality of the communication and of the localization that can be obtained (Munafò et al., 2018). Three different MAC schemes have been implemented: Single Access (SA), Time-Division Multiple Access (TDMA), and Carrier-Sense Multiple Access (CSMA):

Single Access can be used to support scenarios in which one node has exclusive access to the communication channel. This can, for example, be used to support the operation of a LBL-like interrogation. Under this method, each node interrogates (pings) every other node in the network and waits for a reception acknowledgement. To make it possible for more than one vehicle to transmit, it is possible to configure the nodes to take turns to act as interrogators as similarly done in TDMA (see below). The main difference with respect to the more generic TDMA MAC is that there is no explicit time slot assigned to the nodes, so that the interrogated nodes can reply right away to point-to-point requests. This reduces the turnaround time of the reply and improves the localization. Note also that while this method is conceptually similar to a classic LBL, the interrogation in this case does not rely on the physical layer, and it is implemented at network level: it is the network localization layer that generates the required messages as needed (see also Section 2.1.2).

Time-Division Multiple Access is a protocol with a long history of successful application in terrestrial networks, satellite communication systems (Zorzi and Chockalingam, 2003; Peterson, 2003), and underwater networks (Ferri et al., 2017). According to this scheme, different communication nodes share the same bandwidth but they avoid conflicts transmitting at different times. Time is divided into slots that are assigned to the various nodes so that each node can only transmit within its own slot, and it must remain idle in all the other slots. The sum of the set of slots is called *TDMA frame* and it is repeated when it reaches its end. Guard times between slots are needed to avoid overlapping of transmissions and receptions given the long propagation delays. In order to work, TDMA assumes that the all network nodes are clock synchronized. Typically, TDMA works well for small networks in relatively confined areas where the propagation delays are short and the impact of the necessary guard times is limited.

Carrier-Sense Multiple Access is another well-known protocol for channel access (Basagni et al., 2012). According to the CSMA protocol, when a node has a data packet to transmit, it must first check whether the channel is idle or busy. If the channel is idle, it can start packet transmission right away. If the channel is busy, the node must delays its transmission according to an exponential back off mechanism before verifying the channel state again. An optional inter-transmission delay can be also specified to control the throughput of the network. CSMA does not need to use specialized control messages to reserve the channel or to avoid collisions, and for this reason has a very low overhead. Moreover, since each node can verify the channel state and back off when needed independently from each other, CSMA does not require time synchronization. For these reasons, CSMA tend to be more reactive and work better in cases where the size of the deployment area or the number of the nodes is big, as it can rely on the geometric diversity of the network to reduce collisions.

Application layer

The network interacts with the rest of the system through a reception and a transmission interface (inbox/outbox). When a new message is received, the communication service makes it available

through the inbox interface, advertising the availability of the message to any potentially interested application.

On the other hand, when applications want to transmit via the acoustic modem, they encode the messages and associate them with a priority level (0=minimum, 1=very low, 2=low, 3=medium, 4=high, 5=very high, and 6=maximum) and a time to live (TTL). Messages are then published to the network outbox, where they are buffered into an internal queue and sorted according to a defined priority. The queue gets periodically refreshed to remove messages that became stale as their lifetime expired. Every time the MAC policy enables the node for transmission, the message with the highest priority is extracted from the queue and forwarded to the lower layers where it is prepared for acoustic transmission.

In its simplest definition, the sorting priority is static and equal to the priority level associated with the message m:

$$\text{priority}_m(t) = \text{priority}_m = k \in \{0, \dots, 6\}. \tag{1}$$

This has the disadvantage that some messages could never be scheduled for the transmission if one or more applications constantly require the transmission of messages with higher priority. To overcome this issue, the sorting priority can be dynamically adapted using an aging mechanism that takes into account the remaining lifetime of the message m:

$$\text{priority}_m(t) = k + \alpha e^{-\lambda(t_m^e - t)}, \tag{2}$$

where t_m^e is the expiration time of the message m and the parameters $\alpha > 0$ and $\lambda > 0$ can be chosen to shape the time-based term of the sorting priority as desired.

2.1.2. Localization service

The aim of the localization service is to leverage networked communication to obtain localization data. Navigational requirements are linked in this way to the constraints of the acoustic communication. The localization service includes a set of algorithms, each one providing specific localization data (e.g., ranges, bearings, etc.). These can be obtained relying on modem built-in capabilities, or developing an additional layers on top of them. If needed, new localization algorithms (also referred to as localization providers in the following) can be developed and easily added to the system.

The implementation of localization algorithms might require to share information (e.g., own position estimate) with other network nodes. This is done at the network level opportunistically, using regular traffic as much as possible: when a new message is scheduled for transmission (e.g., node status message), the localization provider adds any needed data to the payload, when the available space allows it. The amount of data that can be piggybacked depends on the specific message that is transmitted and on the packet size. On the receiver side, this additional localization information is kept at the localization service level and removed, when present, before forwarding the remainder of the message to the upper layers of the network (i.e., applications). The extracted data are then used by the provider to compute the localization data, and by the network topology reconstruction module, whose function is to collect all the available information about the position of the networks nodes and make this map available locally. This mechanism has the advantage of making the acquisition of localization data transparent to the autonomy system. Furthermore, it ensures that the localization service does not (or has a minimal) impact on the load of the network, nor on the scheduling of regular traffic: no localization-specific message is usually sent through the network. The only exception is represented by the case in which a node has no messages scheduled for transmission. In this situation, the localization provider can be configured to send a localization-specific packet in lieu.

To incorporate in each algorithm the unavoidable delays that the MAC introduces in the system, the localization service is placed between the data-link and the physical layers, as shown in Figure 2. In this way, the localization provider is guaranteed to be executed just before transmitting the message to the acoustic channel. Having a tight coupling between the localization provider and the physical layer allows a more accurate calculation of time intervals between receptions and transmissions, considering that the delay introduced by the piggybacking is usually negligible.

The rest of the paper limits the localization service to the case where the nodes are equipped with acoustic modems, and hence able to measure only the propagation time of acoustic transmissions. This does not limit the generality of the approach, and when more complex devices, such as USBL are available, the system can easily be extended to exploit the additional information. For the purposes of this work, the interface between the localization service and the rest of the system (mainly the navigation system) is hence assumed to be defined by a range measurement and the position of the remote node it refers to.

Two ranging algorithms have been implemented in the localization service. The first is the classic point-to-point LBL-like interrogation; the second is the more flexible network-based interrogation algorithm presented in (Munafò and Ferri, 2017) and referred to as Net-LBL. For completion, both algorithms are briefly reported here.

LBL This method relies on the modem built-in ranging capability to perform a sequential interrogation of the nodes in the network, where unicast messages with acknowledgment are sent to each remote node separately. As soon as the request reached the receiver, a built-in acknowledgement reply is automatically sent by the acoustic modem of the receiver, minimising the turn-around time (TAT). It is worth remarking that, even if the ranging algorithm is embedded in the physical layer, the sequence of the interrogations is established at the network level. This increases the flexibility of the system and makes it possible for the interrogation cycle to adapt to changes in the environment or in the mission. The position of the receiver node can be either preconfigured on the transmitter node (e.g., moored beacons), or sent back to the transmitter by the receiver's localization service as part of a subsequent message. Note that this interrogation method does not scale well with the number of nodes as one interrogation request must be transmitted to each receiver participating in the localization.

Net-LBL The acoustic modems are set up for broadcast transmissions, so that each node can transmit to every other receiver within its maximum communication range. Each node responds to the interrogation according to the selected MAC and sending a message which includes its latest estimated position if underwater, or its latest GPS location if available. Net-LBL leverages the MAC protocol to send the reply, and the localization service to encode the necessary information to be sent back to the interrogator, minimising the number of necessary messages and complying with the operation of the MAC. Note that the usage of broadcast transmissions makes this method to scale with the number of nodes since a single interrogation is required independently of the number of receivers. According to the Net-LBL protocol, each node does not need to have a synchronized clock, as long as the acoustic modem is able to transmit at scheduled times, and information on its local clock is included in each packet. Figure 4 shows a Net-LBL transmission between two nodes. At time $t_0^{(1)}$, node 1 transmits its message to node 2. Node 2 receives the message and saves the time of reception

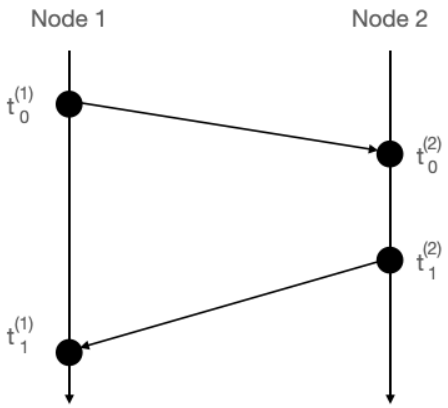

Figure 4. Net-LBL message exchange.

$t_0^{(2)}$ according to its local clock. Node 2 cannot transmit its reply at once, since it has to wait for the node N1's slot to finish. At time $t_1^{(2)}$, Node 2 transmits its response back to node 2. This message includes the message TAT $\delta_{12} = t_1^{(2)} - t_0^{(2)}$ from its last message reception and the current message transmission. When, at time $t_1^{(1)}$ Node 1 receives the message, it is able to calculate the round trip time $RTT_{12} = t_1^{(1)} - t_0^{(1)} - \delta_{12}$ between its initial transmission and the reception of the response. The TAT δ_{12} depends on the specific MAC used and this has a direct impact on the frequency of navigational updates that each node can have (Śliwka et al., 2017). When more nodes are present this scheme can be scaled appropriately using broadcast transmissions. The interested reader is referred to (Munafò and Ferri, 2017) for more details on the Net-LBL interrogation method.

It is worth remarking that, thanks to the fact that the localization is implemented as a network service, independently from the ranging algorithm employed, the localization service can dynamically adapt to changes in the size of the network with no reconfiguration needed (e.g., from an operator). Nodes can enter (e.g., a new vehicle is deployed) or leave (e.g., because of a fault, or loss of the communication link) without disrupting the functioning of the system, causing at most a degradation in its performance (e.g., not enough vehicles to triangulate unambiguously). Note that the performance of each ranging algorithm is strongly dependent on the specific constraints imposed by the MAC protocol. For example, if TDMA is used, the transmission of the response must wait for the next transmission slot. The relation between different MAC protocols and the achievable localization performance is discussed, among others, in (Munafò et al., 2018).

2.2. Acoustic-aided navigation

The acoustic range measurements provided by the localization service are integrated together with proprioceptive data of each node to solve the self-localization problem when the GPS is not available (e.g., when the vehicle is submerged).

As often done in the underwater domain, the localization problem is carried out in the horizontal plane of the local geodetic coordinate system only, given that the depth of each node can be reliably measured using a pressure sensor. Under this assumption, the position of the ith node in the North-East (NE) reference frame $\boldsymbol{x}_i = [x_i,\, y_i]^T$ can be propagated from time k to time $k+1$ using a simple kinematic model (dead-reckoner) that exploits the surge speed v_i and the heading θ_i:

$$\begin{aligned} x_i(k+1) &= x_i(k) + v_i(k)\cos\theta_i(k)\,dt + \nu_x \\ y_i(k+1) &= y_i(k) + v_i(k)\sin\theta_i(k)\,dt + \nu_y \end{aligned}, \tag{3}$$

where dt is the sampling time.[1]

The heading angle is assumed to be measured on-board each node by means of a compass, and to be affected by a noise, modeled as a white, Gaussian random variable with zero mean and variance Q_θ:

$$\theta_i = \bar{\theta}_i + \nu_\theta, \quad \nu_\theta \sim \mathcal{N}(0, Q_\theta). \tag{4}$$

The system assumes that no specific sensor is available (e.g., DVL, and estimates the surge speed from the rotational speed ω_i of the propeller using a constant linear model:

$$v_i = K_{\text{prop}}\,\omega_i + \nu_v, \quad \nu_v \sim \mathcal{N}(0, Q_v), \tag{5}$$

where the constant K_{prop} can be experimentally characterized through tank tests. An additive white, Gaussian noise with zero mean and variance Q_v is also considered to affect the measure.

Note that using such a model, the quantity v_i represents the *surge speed over water* rather than the surge speed of the vehicle, as assumed in (3). This means that the propagation of the position

[1] Hereafter, the indication of the time instant will be omitted in the equations, under the assumption that all quantities refer to time instant k when not otherwise specified.

is subject to drifts in presence of environmental perturbations such as water currents, wind, etc. Fictitious Gaussian process noises ν_x and ν_y with zero mean and variance Q_x and Q_y, respectively, are added in (3) to take into account these unmodeled dynamics (Simon, 2006).

The estimate of the node's position can be refined using the acoustic range $r_{i,j}$ from node i to node j, and the position of jth node $\boldsymbol{x}_j = [x_j, y_j]^T$:

$$r_{i,j} = \sqrt{(x_i - x_j)^2 + (y_i - y_j)^2} + \eta_r, \tag{6}$$

where $\eta_r \sim \mathcal{N}(0, R_r)$ models the noise affecting the range measurements. It is worth nothing that $r_{i,j}$ in Equation (6) represents the distance between the nodes i and j in the horizontal plane (2D), and it can be obtained from the three-dimensional range ${}^3r_{i,j}$ provided by the localization service as follows:

$$r_{i,j} = \sqrt{({}^3r_{i,j})^2 - (z_i - z_j)^2}, \tag{7}$$

where z_i and z_j are the depth of the ith and the jth node, respectively.

When available, the GPS position $\boldsymbol{p}_i$ can also be used to improve the self-localization of the node i. Assuming that the GPS position is affected by a Gaussian noise $\boldsymbol{\eta}_p$ with zero mean and covariance matrix $\boldsymbol{R}_p \in \mathbb{R}^{2\times 2}$, the GPS measurement can be modeled as follows:

$$\boldsymbol{p}_i = \boldsymbol{x}_i + \boldsymbol{\eta}_p. \tag{8}$$

The measurement fusion is done using an Extended Kalman Filter (EKF), where the prediction phase is performed using Equation (3) and the correction step is done with Equations (6) and (8) when the corresponding measurement is available. To mitigate the impact of potential bad measurements on the localization estimate, an outliers filtering technique, called robustifying recursive Least Squares for Additive Outliers (rLS.AO), has been included in the navigation filter (Ruckdeschel et al., 2014). The approach followed by the rLS.AO aims at integrating a measurement z into a Kalman-based observer in order to make the estimation robust to outliers. To do this, the update step of the Kalman filter is modified by applying a saturation $H_b(\boldsymbol{x}) = \boldsymbol{x}\min\{1, b/\|\boldsymbol{x}\|\}$, defined for some suitable upper bound b and norm (e.g., Euclidean norm), to the correction term $\Delta\hat{x}_k = K(z_k - h(\hat{x}_{k+1|k}))$, where K_k is the Kalman gain matrix. The update step of the Kalman filter thus becomes:

$$\hat{x}_{k+1|k+1} = \hat{x}_{k+1|k} + H_b(\Delta\hat{x}_k). \tag{9}$$

The bounding threshold b can be thought as a trade-off between the loss of performance with the respect to the classic Kalman-based estimator in the nominal case (i.e., no outliers) and the benefit gained from the added robustness in presence of outliers. In (Ruckdeschel et al., 2014) two proposals are provided for the choice of b; for the application considered in this work, given the state model (3), the value of b has been intuitively chosen to represent the maximum displacement of the node that the filter will allow following an observation. Note that no modification is applied to the covariance update, since it would only provide a minor gain (Ruckdeschel et al., 2014). The performance of the selected method has been experimentally evaluated over other state-of-the-art outliers filtering techniques, showing less sensitivity to the EKF tuning parameters for this particular application (Fenucci and Munafò, 2020). Finally, it is worth remarking that potential sources of errors in Equation (6) are represented by range measurements $r_{i,j}$ and by the location of the remote beacons $\boldsymbol{x}_j$. The outlier filtering algorithm is hence effective at mitigating not only bad range measurements, but also large and erroneous deviations of the position of the remote beacons.

2.3. ecoSUB vehicles

The platforms employed in this work as nodes of the acoustic network described in Section 2.1 are the ecoSUB vehicles. Three variants have been developed by Planet Ocean Ltd in collaboration with the National Oceanography Centre (Phillips et al., 2017): the smaller 500 m-rated ecoSUBμ5 and

Table 1. Principle parameters for the pre-production ecoSUBμ5 and ecoSUBm5 units utilized

	ecoSUBμ5 V4	**ecoSUBm5 V3**
Depth Rating	500 m	500 m
Dry Weight	$<$ 4 kg	$<$ 12 kg
Length Overall	912 mm	1000 mm
Diameter	111 mm	146 mm
Navigation Sensors	Bosch BNO055 9-axis Orientation Sensor Keller Pressure Sensor PAA-11LX / 50bar Venus638FLPx GPS (Surface Only)	Bosch BNO055 9-axis Orientation Sensor Keller Pressure Sensor PAA-11LX / 250 bar Venus638FLPx GPS (Surface Only) Valeport Altimeter: 500 kHz
Battery Technology	Manganese Alkaline (8S D Cells)	Manganese Alkaline (7S2P D Cells)
Range (predicted)	50 km (Manganese Alkaline)	50 km (Manganese Alkaline)
Maximum Speed	1 m/s	1 m/s
Payload Options	Star Oddi: CT (Huang et al., 2011) NOC: CTDO Valeport: Speed of Sound Newcastle University: Nano Modem	Star Oddi: CT Valeport: Hyperion Fluorometer (Fluorescein, Chlorophyll or Hydrocarbon) Valeport: Fast Response Temperature Newcastle University: Nano Modem GoPro Camera

Figure 5. Fleet of ecoSUBμ5 and ecoSUBm5 prior to a deployment.

two larger variants the 500 m-rated ecoSUBm5 and the 2500 m-rated ecoSUBm25. Details of the pre-production variants used in this project are presented in Table 1 and pictured in Figure 5.

The hull shape of all ecoSUBs variants is based on Myring equations (Myring, 1976) giving an axis-symmetric shape with a ducted propeller and vertical rudder at the rear. These vehicles are under actuated, they utilize an aft propeller for forward thrust, a moving-mass mechanism to control pitch, and a rudder to control the yaw angle. Each vehicle is ballasted to be slightly positively buoyant to ensure that the vehicle's antenna is clear of the water when stationary on the surface, and to increase the probability of the vehicle returning to the surface in the event of a failure whilst

submerged. The pitch of the vehicles is controlled by changing the longitudinal centre of gravity of the vehicle. This is achieved by moving the battery carriage forward and aft on a set of rails using a linear actuator equipped with position feedback. Subject to correct vehicle ballasting, movement of the moving mass is able to induce pitch angles from −80° (nose down) to 70° (nose up). For the ecoSUBμ5, this enables the antenna to be raised nearly vertically in the air.

A limited set of low-cost, low-powered navigation sensors are installed in the ecoSUBs as standard. The vehicle orientation is measured with a Bosch BNO055 nine-axis Orientation Micro-Electro-Mechanical System (MEMS) Sensor, which integrates a triaxial 14-bit accelerometer, a triaxial 16-bit gyroscope with a range of ±2000° per second, a triaxial geomagnetic sensor and a 32-bit microcontroller running Bosch BSX3.0 FusionLib software (Bosch Sensortec, 2020). The vehicle's depth is inferred from a Keller absolute pressure piezoresistive pressure transducer (PAA-11LX) with an error band of <0.05% full scale. To acquire GPS positions fixes whilst on the surface, ecoSUBs are fitted with a Venus638FLPx (SkyTraq Technology, Inc., 2011) GPS unit. Depending on the specific application, additional payload sensors can be fitted on-board each variant; supported devices are listed in Table 1. For this particular application, the nano-modem developed at Newcastle University has been mounted on each variant of the ecoSUBs; refer to Section 2.4 for further details.

Finally, the on-board software is hosted by an Intel Edison which is equipped with a dual-core, dual-threaded Intel Atom Central Processing Unit (CPU) at 500 MHz and a 32-bit Intel Quark microcontroller at 100 MHz (Intel, 2021).

On-Board Control System

Figure 6 illustrates the conceptual block diagram of the ecoSUB on-board software architecture, which is based on the front-seat/back-seat paradigm (Eickstedt and Sideleau, 2010). In the classic front-seat/back-seat paradigm, the vehicle control (the front-seat) and the vehicle autonomy system (the back-seat) are separated: the autonomy system provides high-level set-points (e.g., heading, speed, depth) to the control system, whereas the vehicle control system executes the control and

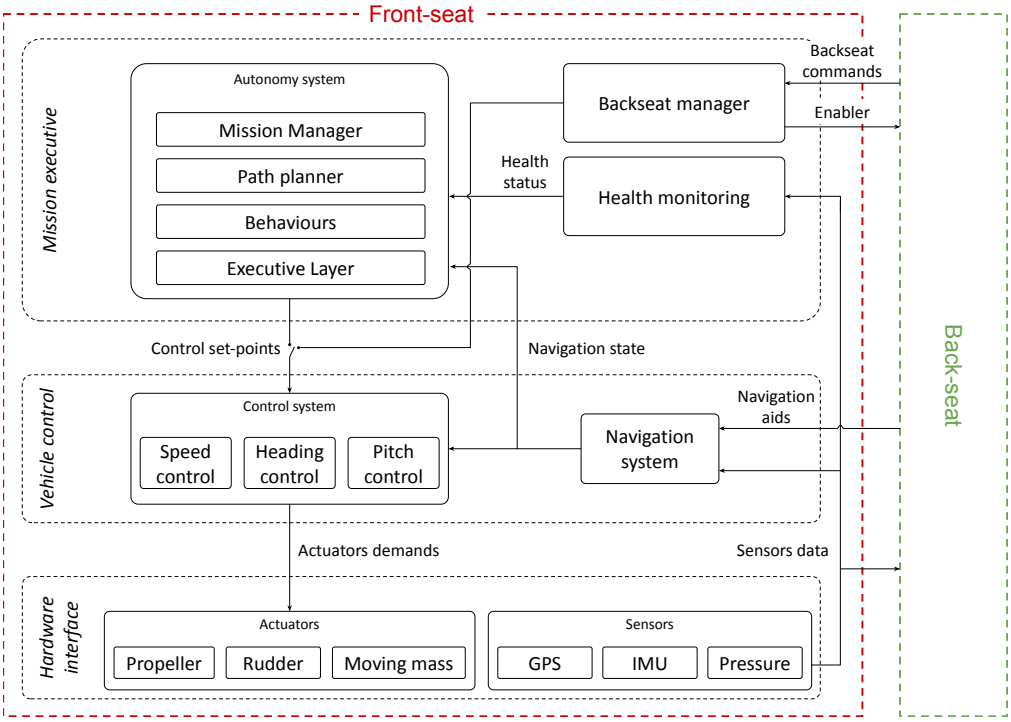

Figure 6. Conceptual block diagram of the ecoSUB software architecture, based on the front-seat/back-seat paradigm.

passes navigation information back to the autonomy system. In contrast with the classic abstraction, the separation between the front-seat and the back-seat in the ecoSUB software architecture aims at preserving the safety of the vehicle. The front-seat provides key functionalities to execute typical underwater missions while guaranteeing the safety of the vehicle, whereas the back-seat allows the definition of additional, user-defined algorithms and behaviours to enhance the vehicle's capabilities and meet specific user and/or mission requirements. Sensors data are made available to the back-seat and can be exploited to produce commands for the control system (effectively allowing the back-seat to drive the vehicle) and/or additional aids for the navigation system. The front-seat can grant and revoke the control of the vehicle to the back-seat. Control set-points coming from the back-seat are filtered in the front-seat before being forwarded to the control system: this way, the execution of arbitrarily defined behaviours can be prevented in case they violate the safety measures established for the vehicle. Analogously, in case a condition of imminent danger is dynamically detected, the front-seat can take back the control of the vehicle, e.g., to execute emergency behaviours.

In particular, the front-seat is a three-layered system consisting of a hardware interface layer, a vehicle control layer, and a mission executive. The *hardware interface* layer is composed of a set of software modules, each one acting as the "driver" of the device (i.e., a sensor or an actuator) it is associated to. The *vehicle control* layer is responsible for carrying out the low-level control and the navigation tasks. The mutual interaction between these two layers provides the vehicle with basic motion capabilities: on one hand, sensor drivers acquire data from the corresponding device and forward them to the main navigation system, implementing a simple Dead-Reckoning (DR) algorithm; on the other hand, actuator drivers receive the commands computed by the control system and send them to each actuator to move the vehicle. Finally, the *mission executive* includes a autonomy system that enables the execution and the monitoring of mission plans through a set of predefined behaviours of common use (e.g., "go to depth" - depth controller, "go to lat./lon." - line-of-sight guidance law, etc.). Behaviours can be combined together to obtain more complex behaviours: for instance, the "go to waypoint" behaviour is obtained composing the "go to lat./lon." and the "go to depth" behaviours running in parallel. In the same way, the "lawn-mower" behaviour is obtained as a sequence of "go to waypoint" behaviours to each waypoint defining the lawn-mower path. To manage the shifting of control authority between the front-seat and the back-seat, the mission executive includes a back-seat manager, which is responsible to verify that all commands received from the back-seat comply with desired safety requirements. From an implementation perspective, the ecoSUB front-seat is implemented in Robot Operating System (ROS) (Quigley et al., 2009), running on top of the ubilinux 2.0 operating system.

Surface station keep behaviour. For the purpose of this work, a new behaviour has been developed to manage the vehicle station keeping on the surface. When an ecoSUB vehicle is on the surface to act as an anchor node, it raises its antenna out of the water to connect to GPS and Iridium, and lowers the acoustic modem. While this configuration maximizes the vehicle connectivity, it effectively limits its manoeuvrability, leaving the vehicle to drift with winds and currents. The behaviour monitors the vehicle location, and triggers a transit back to the desired position when the node drifts out of a user defined acceptance radius. To maximize efficiency the transit towards the target waypoint is done submerged: travelling underwater makes it possible to decrease the impact of disturbances such as sea-waves and wind-induced currents on the vehicle motion. It is important to point out that during the short underwater transit, the position of the vehicle is continuously dead reckoned. The expected degradation in the precision of the position estimate is typically such that the vehicle can continue serving as a reference beacon. In those cases where the accumulated dead reckoned position error is higher than expected, the outlier filter mitigates the effect of such errors as discussed in Section 2.2. The behaviour and its effects on a surface node is shown in Figure 7. The pseudo-code algorithmic description of the behaviour is reported in Algorithm 1. A PID controller is used to calculate the desired forward speed and heading to re-enter the desired acceptance radius. Two different acceptance parameters are used: ρ is used to determine when the vehicle is outside the desired acceptance region, and $\psi < \rho$ to determine when a waypoint is considered to be reached.

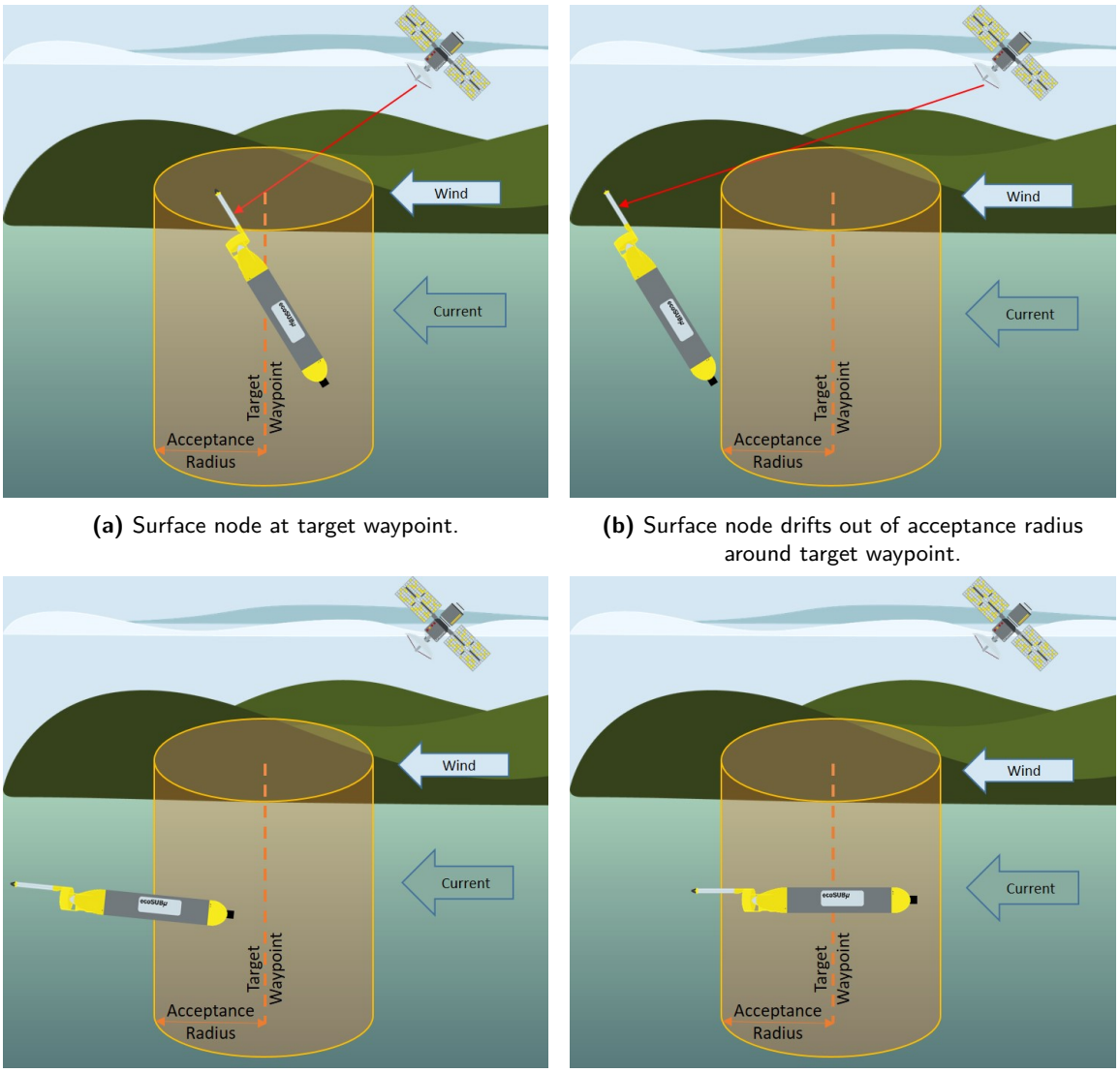

(a) Surface node at target waypoint.

(b) Surface node drifts out of acceptance radius around target waypoint.

(c) AUV dives and transits back towards the target waypoint.

(d) At the target waypoint the AUV stops and returns to the surface.

Figure 7. "Station keeping" behaviour of AUVs primarily acting as surface nodes.

2.4. System integration

Each of the AUVs utilized in the network was fitted with a nano-modem electronics PCB, mounted inside the main pressure vessel and connected via RS232 to the transducer. For the ecoSUBμ5 the modem transducer has been mounted as part of the 3D printed nose, and aligned with the main axis of the vehicle so the modem transducer is pointing vertically down when the AUV is acting as a surface node (see Figure 8a). On the ecoSUBm5 vehicles the transducer is mounted in the nose but pointing vertically up as shown in Figure 8b. This configuration has been chosen for two main reasons: (a) leaves enough room inside the nose of the vehicle to install an additional single beam echo-sounder that can be used to gather bathymetric data and (b) provides a stable acoustic link when the vehicle is underwater. Note that while these two configurations define a level of specialization for the vehicles, this is only due to hardware constraints and it does not limit the flexibility of the network services provided. This difference however is used at the autonomy level,

Algorithm 1. Surface station keep behaviour

input : $\boldsymbol{x} = [x,\ y]^T$, vehicle position;
$\boldsymbol{x_d} = [x_d,\ y_d]^T$, target waypoint;
ρ, area acceptance radius;
ψ, waypoint reached acceptance radius.
output: u, forward speed;
θ, heading
while stationKeepRequired **do**
  $\epsilon = \|\boldsymbol{x_d} - \boldsymbol{x}\|$;
  $\epsilon_\theta = \text{acos}\left(\frac{x_d - x}{\|\boldsymbol{x_d} - \boldsymbol{x}\|}\right) - \theta$;
  if $\epsilon > \rho$ **then**
    // Out of acceptance area for $\boldsymbol{x_d}$
    MoveBatteryTo(*Dive*);
    Dive();
    // Calculate speed and heading to get back to the target position.
    u $\leftarrow$ PID(ϵ);
    $\theta \leftarrow$ PID(ϵ_θ);
  else
    if $\epsilon <= \psi$ **then**
      // Waypoint $\boldsymbol{x_d}$ reached
      Surface();
      MoveBatteryTo(*Front*);
      u = 0;
    end
  end
end

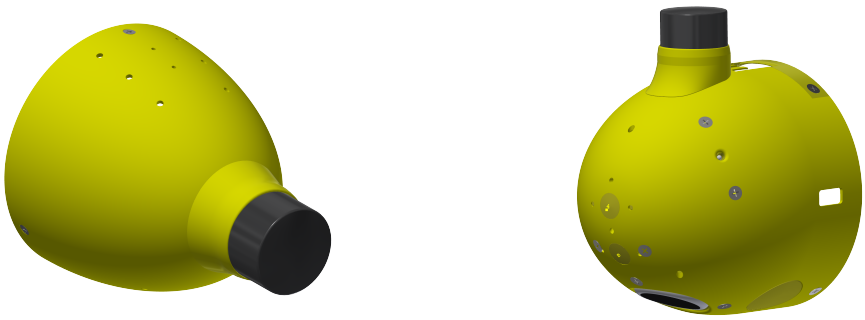

(a) ecoSUBμ5. **(b)** ecoSUBm5.

Figure 8. CAD design for the integration of the miniature acoustic modems on ecoSUB vehicles.

with different missions assigned to different vehicles based on the available sensors (e.g., vehicles equipped with echo-sounders are used to perform bathymetric surveys).

The system described in the previous sections has been implemented as back-seat (see Section 2.3) ROS software modules (also referred to as *ROS nodes*) and integrated with the vehicle front-seat control system to provide the vehicle with communication, networking and enhanced navigation capabilities. The front-seat/back-seat separation of responsibility and their main interactions are reported in Figure 9. One ROS node is responsible of interacting with the firmware of the acoustic modems, acting as the driver of the device in the back-seat architecture. A second module, called the network manager, implements the rest of the network stack. To accommodate for the specific needs that different applications or deployments may require, the channel sharing protocol, as well as the acoustic ranging algorithm can be selected and configured before launching the vehicle.

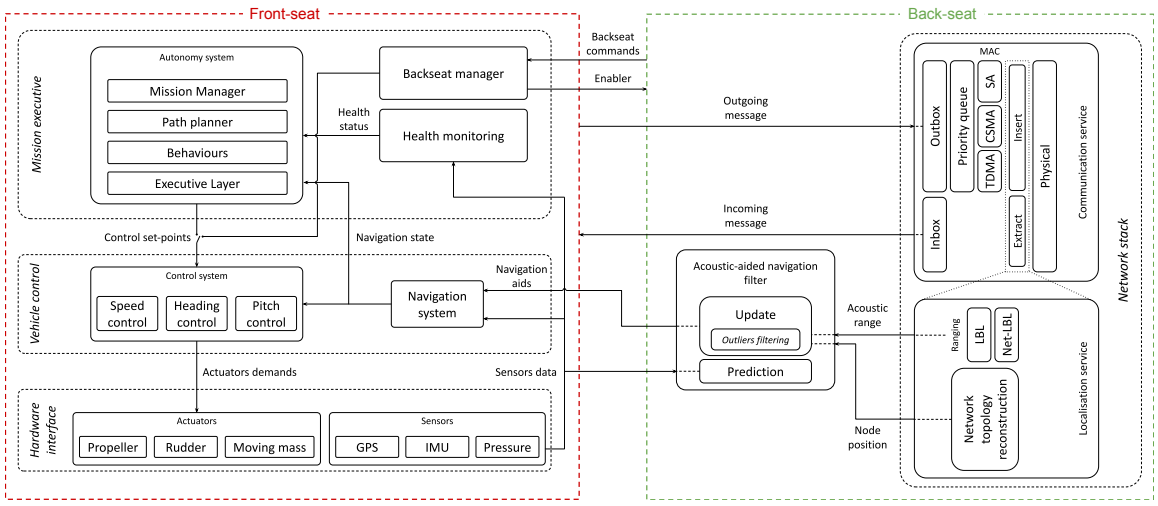

Figure 9. Software architecture developed for the integration of the proposed networked navigation system with the on-board ecoSUB system.

Moreover, the network manager is designed to easily support the extension with custom MAC policies, and/or localization services. The message queuing priority is static in the current version of the network manager, but the inclusion of a dynamic sorting priority would be a trivial addition. The acoustic-aided navigation filter completes the set of software nodes running at the back-seat level. Proprioceptive data of the vehicle (speed over water and heading) and GPS measurements are received from the front-seat and integrated, in the back-seat navigation filter, together with network-calculated acoustic ranges to produce an estimate of the vehicle's position. Position estimates are then fed back to the main front-seat navigation system, which updates the navigation solution of the vehicle treating the back-seat estimates as straightforward position measurements, similarly to those provided by a USBL or a GPS.

3. Field Trials

The proposed system was tested during the 11th Breaking the Surface (BtS) workshop (University of Zagreb, 2021), held in Biograd Na Moru, in the area of Zadar, Croatia, between the 29th of September and the 5th of October 2019. The aim of the trial was to demonstrate the efficiency of the network based localization in two scenarios: firstly, with anchored surface nodes in a confined body of water, and secondly, with mobile surface nodes in open waters. The Straits around Zadar are a particularly suitable environment to validate the system proposed in this work, with circulation patterns perturbed by higher-frequency current variations. Winds, amplified by islands and topography, are an important driving force in the straits, resulting in currents larger than usual in the Mediterranean Sea (Orlic et al., 1992).

3.1. Trials in Confined Waters

Trials in confined waters where conducted between the 30th of September and the 3rd of October 2019 in the region enclosed by Beach Dražice, a 250 m gently sloping pebble beach which reaches a maximum depth of approximately 10 m (Figure 10, Region 1, green box). The objectives were to (a) demonstrate the functionality of the system as the number of nodes of the network increase, and (b) assess the robustness and the long-range capabilities of the acoustic-aided navigation in controlled conditions. Two specific missions, M1 and M3, were performed to experimentally validate the system.

Figure 10. Geolocalization of the working sites of the BtS experimental campaign. The preliminary tests were conducted in Region 1 (green box) from the 30th of September to the 3rd of October 2019. Region 2 (violet box) represented the operative area of the open water tests of the 4th of October 2019.

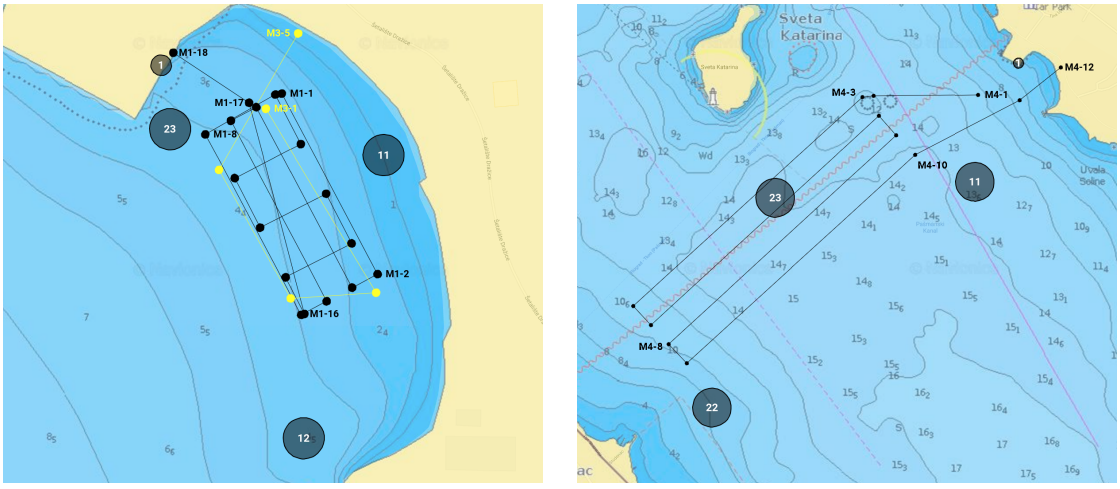

(a) Experimental setup of the missions M1 and M3. **(b)** Experimental setup of the mission M4.

Figure 11. Experimental setup of the missions executed in the BtS campaign.

3.1.1. Mission M1

Mission M1 was done on the 1st of October to evaluate the performance as the network size was increased. During the test, up to seven nodes were deployed. Three of them, represented by ecoSUBμ5 vehicles 11, 12, and 23, were tasked to act as surface gateways. For test M1, the surface vehicles were directly anchored at their desired locations (see black-shaded circles in Figure 11a). This was done to simplify the experimental setup to separate the achievable navigation performance

from the additional complexities due to the station keep behaviour. An additional acoustic modem was connected to the base station and deployed from the land (node 1 in Figure 11a). This modem was set up in promiscuous mode to receive all the network traffic and used for mission monitoring. Finally, three underwater nodes, represented by ecoSUBm5 vehicles 154, 157, and 161, were simultaneously deployed to execute pre-planned lawn-mowing trajectories as shown with the dotted black lines in Figure 11a. Each vehicle was navigating at different depths: 154 at 2 m, 157 at 3 m, and 161 at 4 m, respectively). The mission consisted in two consecutive lawn-mower paths: the first sequence was composed of four 100 m long, 15 m spaced legs directed from North-North-West to South-South-East, starting from waypoint M1-1 up to waypoint M1-8. The second lawn mower path was defined in the same area, from waypoint M1-8 to waypoint M1-16, with legs directed in the perpendicular direction. Finally, the mission included two last legs to bring the vehicle back to the deployment point close to the base station (M1-16 to M1-17 underwater, M1-17 to M1-18 on surface).

3.1.2. Mission M3

Mission M3 was performed on the 3rd of October. The test consisted in multiple runs of the same trajectory to assess the robustness of the networked localization system. The network setup was similar to the one used in mission M1, with the three surface nodes anchored approximately in the same locations, and the base station used for mission monitoring. The underwater nodes were represented by two ecoSUBm5 vehicles (154 and 157), programmed to perform two different missions. ecoSUBm5 157 executed three repetitions of the lawn-mower path defined in mission M1 (Figure 11a, black path) at 2 m depth. ecoSUBm5 154 was deployed multiple times from the base station and commanded to travel at 3 m depth along the trapezoidal-shaped path (Figure 11a, yellow path), starting from waypoint M3-1 up to the recovery point close to the shore corresponding to waypoint M3-5. In the first two runs, the first leg starting at M3-1 was executed on the surface; in the last two runs, ecoSUBm5 154 dived directly at M3-1 and traveled through the entire predefined path at a depth of 3 m.

3.2. Trials in Open Waters

An open water trial was conducted in the Zadar Channel between Biograd Na Moru and Tkon, just South-East of Sveta Katarine island (Figure 10, Region 2, violet box) on the 4th of October 2019. At this location the channel is approximately 2.2 km wide with a sandy / muddy bottom and approximately 15 m water depth over its central section where the trials were conducted. Throughout the experiment a force 3 North-Westerly breeze was present. This experiment, referred to as M4, was the most complex one performed, and its main goal was to demonstrate the ability of the network to support long-endurance and long-range missions.

3.2.1. Mission M4

In mission M4, ecoSUBμ5 vehicles 11, 22, and 23 were tasked to execute the station keep behaviour in three circular areas of $\rho = 75$ m radius. These areas are indicated with black-shaded circles in Figure 11b, together with the ID of the vehicle tasked to station keep. Starting from the location indicated by waypoint M4-1, ecoSUBm5 157 was programmed to cross the channel multiple times at 5 m depth, following a lawn-mower path composed of four 1.5 km long legs, with a 100 m separation one from each other (M4-3 to M4-10, black path in Figure 11b). Finally, two last legs were defined to drive the vehicle to the recovery point M4-12. The base station was deployed on shore, facing the channel (node 1 in Figure 11b). While initially used for mission monitoring only, it was retasked on the fly to act as a surface node and help the ecoSUBm5 157 on its way back from waypoint M4-8.

During the experiment, range measurements were evaluated on-board the underwater vehicles by the network's localization service, using the Net-LBL algorithm described in Section 2.1.2. This choice was motivated by the fact that Net-LBL is generally more scalable than the classic LBL approach. The access to the acoustic channel was granted to each node according to the CSMA protocol, with a minimum inter-transmission delay of 10 s. (Śliwka et al., 2017) reported that for the Net-LBL algorithm, CSMA is a better alternative than TDMA, and that can lead to a 30% average

Table 2. Summary of the network settings for the selected mission runs. One additional node deployed from land was also present to monitor the mission.

Mission ID	Date	Region	Surface nodes	Underwater nodes
M1	1st Oct.	1	11, 12, 23	154, 157, 161
M3	3th Oct.	1	11, 12, 23	154, 157
M4	4th Oct.	2	11, 22, 23	157

Table 3. Summary of the navigation performance of both the EKF and the DR in the selected mission runs.

Mission ID	Vehicle ID	Duration (s)	Distance traveled (DT) (m)	Surfacing error (m)		Surfacing error (% DT)		Error reduction (% DR)
				EKF	DR	EKF	DR	
M1	154	1655	1230	15	48	1.22	3.89	68.75
	157	1315	1000	10	69	1.04	6.94	85.51
	161	1770	1913	16	84	0.84	4.4	80.95
M3	154	595	550	5	23	0.85	4.17	78.62
		575	431	4	16	1.01	3.6	75
		640	464	4	12	0.81	2.63	66.67
		650	540	6	7	1.16	1.35	14.29
	157	3650	2743	9	153	0.05	5.54	94.12
M4	157	12000	9447	25	675	0.27	7.15	96.27

improvement in the localization error, and even up to 90% under optimal conditions. Underwater vehicles were periodically transmitting their navigation state (i.e., position and associated covariance) through the acoustic network for monitoring purposes. To maximize the chances of getting range measurements, the localization service was configured to send a ranging request/reply in case no other message was scheduled for transmission after the MAC enabling. The tuning parameters of the acoustic-aided navigation filter were experimentally determined during preliminary tests performed prior to M1. In particular, the bounding threshold b of the outliers filtering algorithm was set to 10 m. Table 2 summarizes settings and parameters of the underwater acoustic network for each mission.

4. Navigation Performance

This section presents the results obtained in real-time with the proposed collaborative navigation system in the missions M1, M3 and M4. The real-time output of the acoustic-aided navigation filter is compared with the dead-reckoned path reconstructed in post-processing. Due to the lack of a reliable ground-truth for the vehicle position while underwater, the navigation performance can only be evaluated at the surfacing point at the end of each dive. In the following analysis, the performance index will hence be represented by the localization error (i.e., the distance between the estimated and the GPS positions) at the end of each dive. To have a uniform comparison of the performance of the two navigation solutions across the different missions, the surfacing errors have been also normalized with respect to the distance traveled. In the absence of a ground-truth, the reference value to be used as an indication of the distance traveled has been calculated as the sum of the displacements given by two consecutive position estimates provided by the EKF throughout the mission. Table 3 gives an overview of the navigation performance obtained for each vehicle in all the reported missions, whereas Table 4 collects the number of range measurements that each underwater vehicle gathered from each surface node in the selected runs.

4.1. Mission M1

Navigation results for mission M1 are reported in Figure 12, as calculated by the back-seat navigation filter. Overall, all vehicles had relatively low navigational errors (min. 10 m, max. 16 m) when

Table 4. Summary of the ranging statistics in the selected mission runs. The mode has been evaluated rounding the update period to the nearest ten.

Mission ID	Vehicle ID	Total no. of ranges	Surface node ID	No. of ranges	Range update period (s)			
					Avg.	Median	Mode	Std. dev.
M1	154	101	11	40	36.9	29.0	20.0	33.5
			12	32	44.2	28.0	20.0	53.0
			23	29	54.3	35.0	10.0	59.1
	157	119	11	46	26.3	26.0	10.0	18.9
			12	30	39.6	19.0	10.0	42.7
			23	43	27.6	21.0	10.0	22.1
	161	169	11	69	23.1	17.5	10.0	18.0
			12	59	26.6	18.0	10.0	21.0
			23	41	40.0	31.5	10.0	32.8
M3	154	25	11	4	64.3	53.0	10.0	49.6
			12	11	27.7	17.0	10.0	27.6
			23	10	29.2	24.0	10.0	25.2
		30	11	10	22.1	10.0	10.0	22.3
			12	4	29.3	32.0	20.0	10.0
			23	16	18.8	16.0	20.0	12.8
		46	11	17	28.3	17.5	10.0	22.0
			12	10	24.2	21.0	20.0	18.6
			23	19	23.8	14.5	10.0	15.5
		42	11	17	26.9	22.5	20.0	17.4
			12	15	30.6	19.0	20.0	21.1
			23	10	44.2	48.0	10.0	26.1
	157	338	11	91	39.2	25.5	10.0	33.2
			12	91	37.2	20.5	10.0	36.5
			23	156	22.4	11.0	10.0	17.5
M4	157	884	1	71	51.2	21.0	10.0	62.1
			11	58	75.1	11.0	10.0	277.9
			22	128	83.8	10.0	10.0	261.2
			23	627	16.8	10.0	10.0	31.8

compared with the DR. The reconstructed trajectories are shown in Figure 12. It is important to note that during the trials, the vehicles had some minor issues that did not have any impact on the localization experiments, but that did affect the path following of the ecoSUBs. More specifically, ecoSUBm5 154 had a compass malfunction (most likely due to a poor calibration) that was not possible to fully correct on site and that resulted in trajectory over-correction during the activities. This is visible in Figure 12a, with the vehicle oscillating over the desired path. ecoSUBm5 161 had a heading control issue that constrained the turning radius of the vehicle resulting in larger turns around waypoints and more aggressive controls commanded by the internal PID to correct the vehicle behaviour (see Figure 12c). Unfortunately, the source of this error was not fully identified during the trials, and it may have been the effect of multiple, combined issues, including a mechanical defect of the rudder and control related problems. Moreover, ecoSUBm5 161 surfaced twice during the mission (close to the waypoint M1-2 on the first lap, and between the waypoint M1-1 and the shoreline on the second lap). This was due to the fact that the previously described heading issue led the vehicle too close to the shore, and into shallow areas where the altitude safety control forced the vehicle to surface.

Furthermore, mission M1 gives an indication of the scalability of the proposed system. Figure 13 reports the times of arrival of the range measurements collected on-board the underwater vehicles

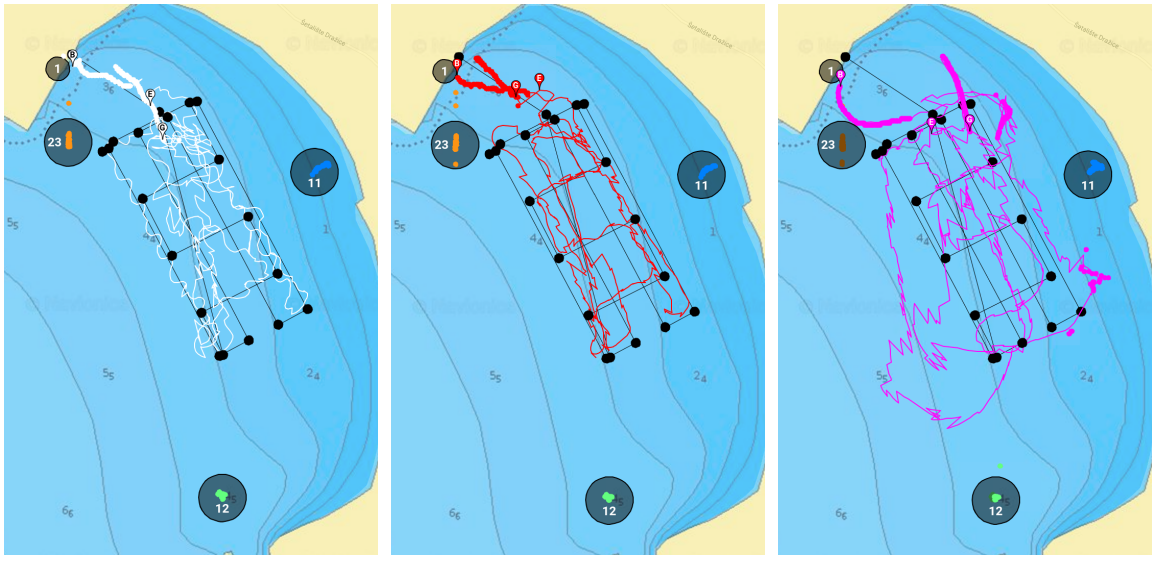

(a) ecoSUBm5 154. **(b)** ecoSUBm5 157. **(c)** ecoSUBm5 161.

Figure 12. Mission M1, localization results. The reference path and associated waypoints defining the mission are shown in black. GPS positions of the surface nodes 11, 12 and 23 are indicated with blue, green and orange circles, respectively. The (a) white, (b) red, and (c) magenta paths represent the position estimated on-line with the proposed navigation system for vehicles 154, 157, and 161, respectively; the underwater part is illustrated with a thin line, whereas positions on surface are indicated with circles. The starting position is marked with a 'B'; the estimated and the GPS-based locations at the surfacing are labeled with a "E" and a "G," respectively.

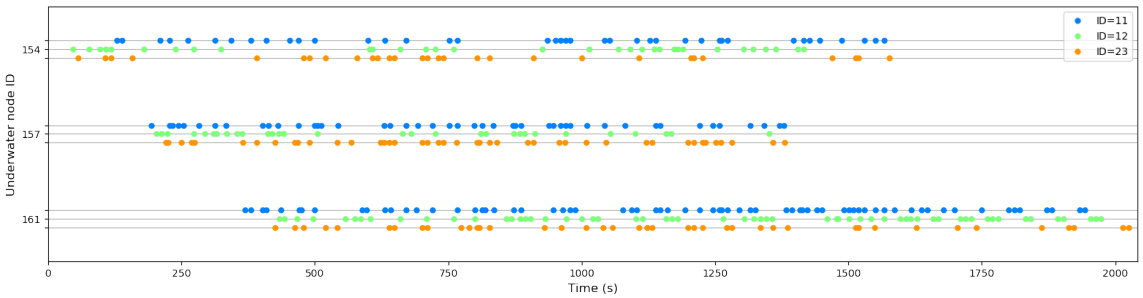

Figure 13. Mission M1, time distribution of range measurements on-board the ecoSUBm5 154 (top), 157 (middle) and 161 (bottom). Data have been synchronized off-line to a common timescale.

during their mission. Data have been synchronized off-line to a common timescale, as the vehicles were not required to have real-time synchronized clocks. It is possible to see that the range distribution does not present substantial differences as the dimension of the network changes. Range statistics reported in Table 4 show that even when the range update period has a higher variability (see column "Std. dev." in Table 4), most ranges are received with an update period of 10 s from each surface node (see column "Mode" in Table 4). Finally, it is possible to calculate the frequency of the range measurements received on-board each underwater vehicle (total range number over mission duration), resulting in one range every about 12 s on average. These numbers are consistent with the inter-transmission time set for the CSMA in this mission, meaning that the network dimension has a minimal impact on the expected communication and ranging performance.

From the results of mission M1 it is hence possible to conclude that the proposed collaborative navigation system (a) is able to outperform the localization obtained with the DR and (b) scales well with the network dimension.

4.2. Mission M3

Results from test M3 are reported in Figure 14. ecoSUBm5 154 was deployed multiple times from the base station 1 and exhibited a consistent behaviour throughout all the repetitions of the programmed mission (Figure 14a). Note again the oscillations in the estimated navigation due to the issue mentioned before. As expected, shorter missions have a lower overall DR navigational error, relatively comparable with the one achieved using the network-generated measurements. However, as the mission duration increases so does the DR navigation error. In fact, the reconstructed DR for vehicle 157 experienced a localization error of 153 m in about 1 h, whereas the network-based navigation constrained the error to 9 m only, similarly to what have been obtained in the previous missions. Figure 15 shows the time distribution of the range measurements collected on-board the two vehicles. Note that in the first two runs of vehicle 154 range measurements were not available at the beginning of the mission, as the first leg of the programmed path was executed on surface, as described in Section 3.1.2.

From the results of mission M3, it is hence possible to conclude that the localization performance of the proposed collaborative navigation system are (a) repeatable in time and (b) bounded within the same order of magnitude regardless of the mission length, in contrast with the error obtained using the DR which grows indefinitely.

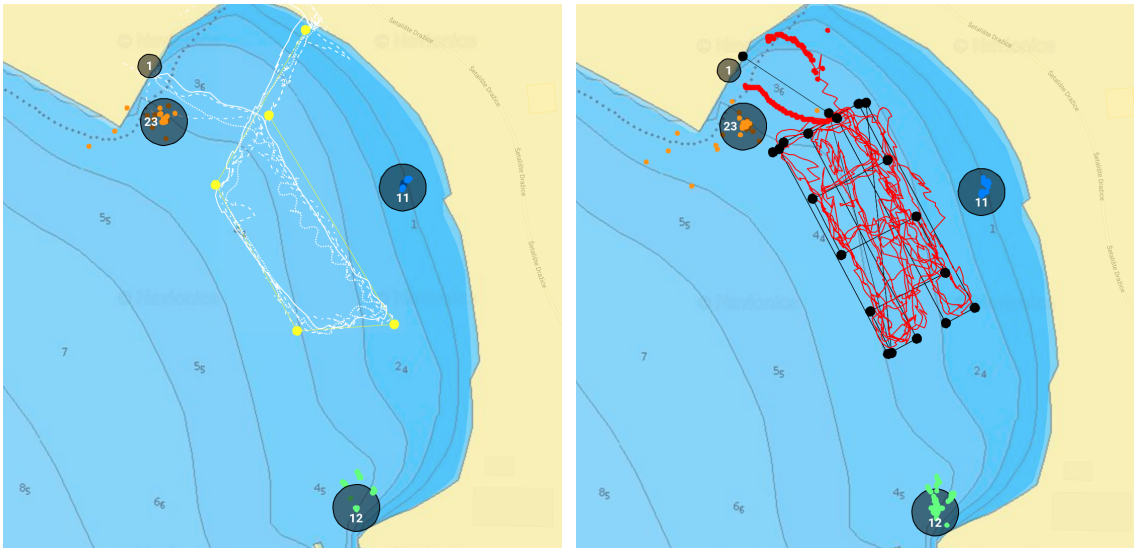

(a) ecoSUBm5 154. **(b)** ecoSUBm5 157.

Figure 14. Mission M3, localization results. The reference paths and associated waypoints defining the mission are shown in (a) yellow and (b) black. For surface and underwater nodes the legend is the same used in Figure 12.

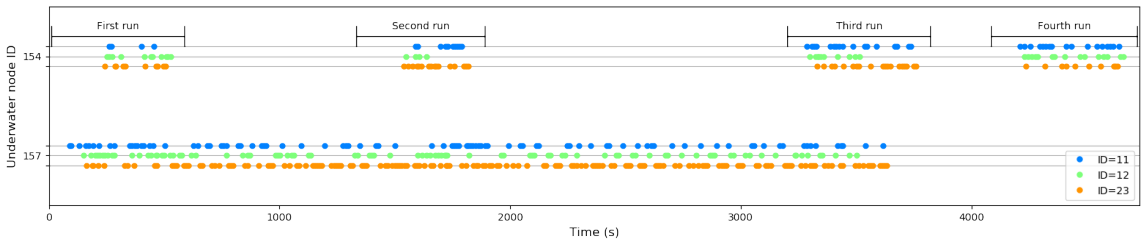

Figure 15. Mission M3, time distribution of range measurements on-board the ecoSUBm5 154 (top), and 157 (bottom). Data have been synchronized off-line to a common timescale.

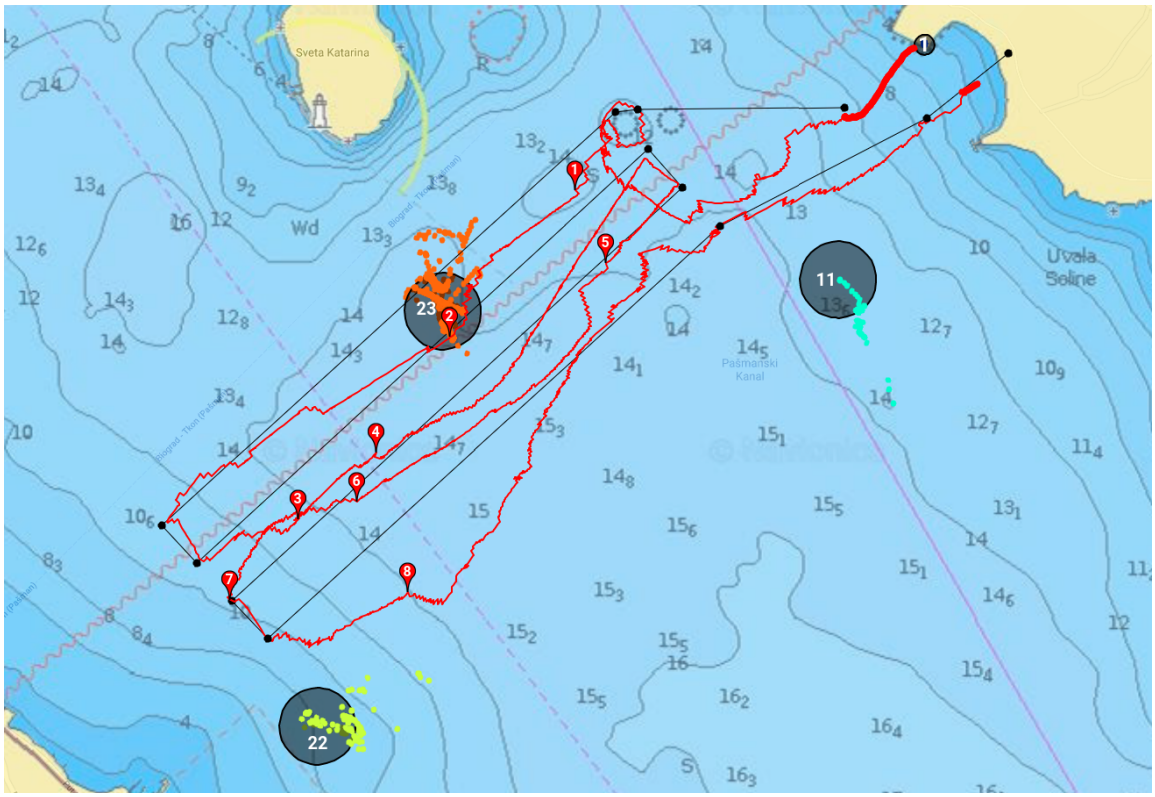

Figure 16. Mission M4, localization results. The reference path and associated waypoints defining the mission are shown in black. GPS positions of the surface nodes 11, 22, and 23 are indicated with cyan, yellow and orange circles, respectively. The red path represents the position estimated on-line with the proposed navigation system for vehicle 157; the underwater part is illustrated with a thin line, whereas positions on surface are indicated with circles. Along the path, eight points of interest are highlighted with markers; refer to the text for more details.

4.3. Mission M4

The outcomes obtained from tests in the confined waters made it possible to set for more ambitious goals for M4, and navigate in open waters across the Zadar channel, approximately 3 km wide. ecoSUBm5 157 was chosen for this mission given the better stability shown in the previous trials. Navigation results are reported in Figures 16 (on-line estimated navigation), 17 (acoustic ranges) and 18 (spatial uncertainty of the navigation (Webster et al., 2012)). The vehicles acting as surface nodes (11, 22 and 23) were able to station keep as required. As it is visible in the example reported in Figure 19, they periodically drifted out of their designated area of operation and replanned their mission to move back inside according to the behaviour described in Section 2.3. When on surface, the vehicles were drifting at approximately 0.2 m/s. Note that 0.2 m/s is a substantial water current for the ecoSUB vehicles, as this corresponds to approximately 25% of the maximum vehicle speed. As soon as the vehicle was outside of the circular area, it started powering back to the centre travelling underwater at 3 m depth. This effect was particularly evident in the initial and the final parts of the mission, when stronger environmental conditions (wind, surface waves) pushed the surface vehicle to drift outside of the designated area more frequently. In the middle part of the mission, the vehicle was able to stay at the surface, within the desired range and with no need for any corrective actions, for more than 4000 s (see between time 8500-12500 s in Figure 19).

ecoSUBm5 157 was deployed close to the base station, navigated on the surface to waypoint M4-1, and then dived to start its underwater navigation. Once underwater the vehicle started to collect range measurements from the surface nodes. As Figure 17 highlights, the availability of range

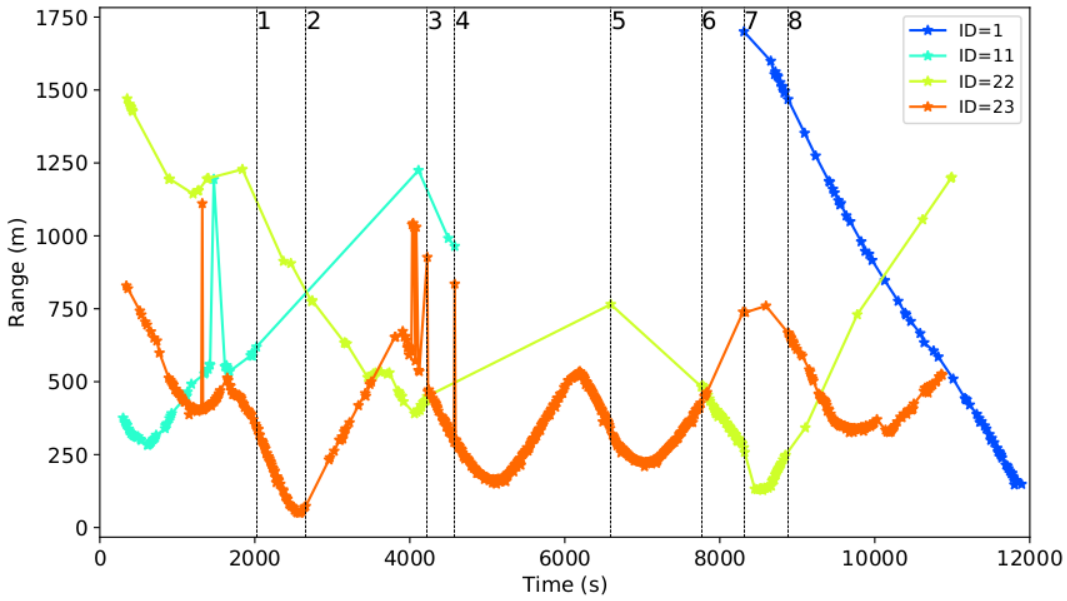

Figure 17. Mission M4, range measurements collected on-board the ecoSUBm5 157. The eight dashed vertical bars highlight the time instants corresponding to the markers in Figure 16.

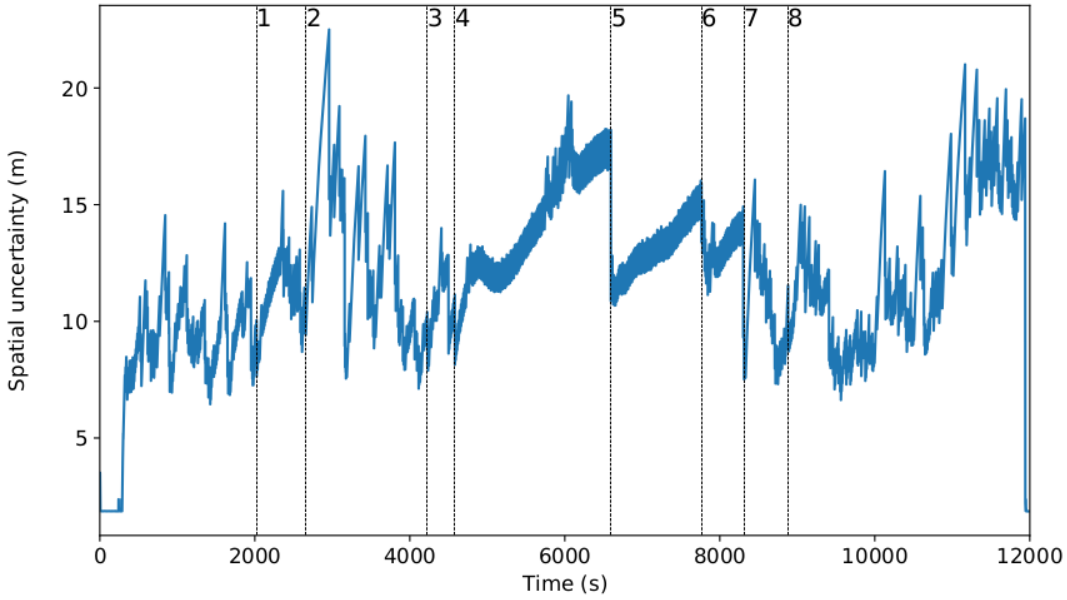

Figure 18. Mission M4, spatial uncertainty of the back-seat navigation filter. The eight dashed vertical bars highlight the time instants corresponding to the markers in Figure 16.

measurements on-board vehicle 157 exhibits some irregularities for each surface node. A smaller number of range measurements were obtained from ecoSUBμ5 22. This node was deployed on the other side of the channel and only reachable when the vehicle was within communication range. This resulted in node 22 to intermittently participate in the network, remaining out of range between markers "3' and "6" (see Figure 17). Soon after vehicle 157 started the first leg of the lawn-mower (marker "1"), ecoSUBμ5 11 experienced a mechanical issue and started to drift with the current, until it effectively went too far away and out of communication range (marker "4," Figure 17).

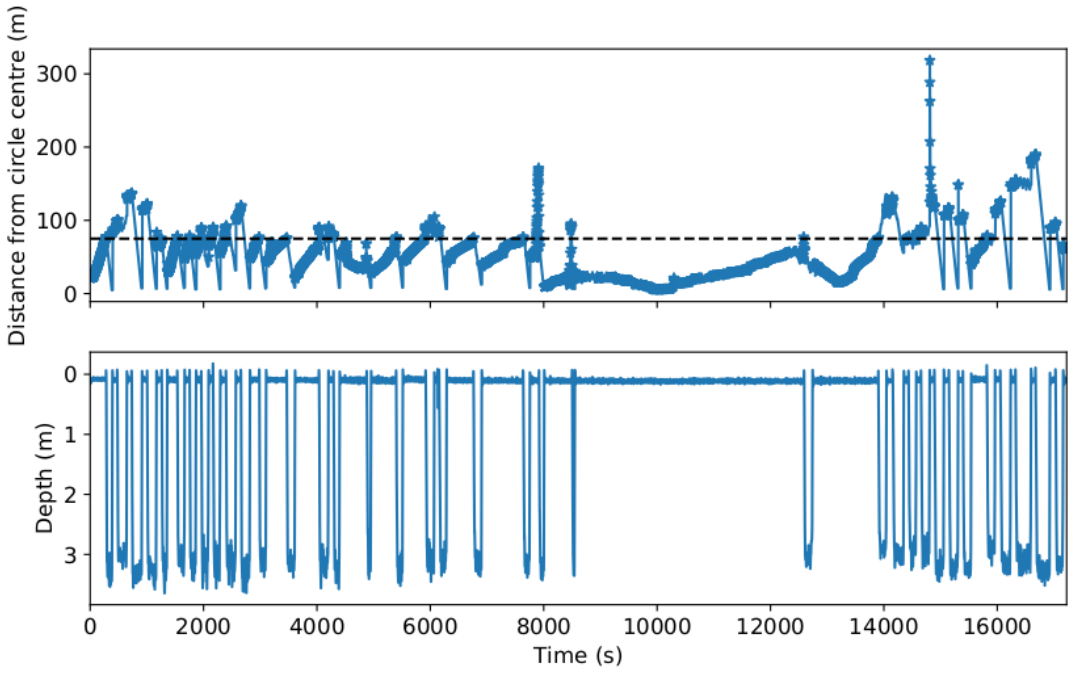

Figure 19. Mission M4, station keep behaviour results for ecoSUBμ5 23. Top: distance from the centre of the circle; the blue dots indicate the GPS availability, whereas the dashed black line represent the desired radius ρ. Bottom: vehicle depth.

Range measurements from node 23 present gaps between markers '2" an "3," and between markers "6" and "8," corresponding to the South-Western region of the mission area (see Figure 16). This could be due to several concurrent reasons which are difficult to pin-point and isolate. A possible explanation could be that the relative geometry made acoustic communications more difficult with node 22. In this region water depth decreases from 14 m to approximately 9 m (see bathymetric contours in Figure 16), making effects such as multipaths and reverberation more likely to happen.

Another possible effect was the masking of the acoustic path from the modem on the vehicle to the one on the remote beacon by the vehicle hull due to the trajectory of the vehicle. The AUV was moving away from the remote node, and when in navigation, to maintain a desired depth, the vehicle pitches down by about 10°. This puts the modem on the vehicle within what could be a partially acoustically shadowed area, and any communication with a node located behind the vehicle might need to mostly rely on surface reflections to be successful. Unfortunately, a complete environmental characterization is not available to properly test these hypotheses.

These combined effects resulted in ecoSUBm5 157 navigating relying on a single beacon (node 23) for about an hour (between markers "3" and "7," Figure 17) of the mission. Figure 18 shows how ranges coming even from a single beacon are able to limit the spatial uncertainty of the navigation estimate, although in only one direction of the horizontal plane. As soon as a range measurement coming from a different anchor is received, the spatial uncertainty drops down (e.g., markers "5' and "7," Figure 18), meaning that the position covariance has been reduced along a different direction. To provide the vehicle with an additional surface anchor on its way back to the recovery point (starting from marker "7"), the monitoring station was reconfigured to act as an additional surface node. It is important to highlight that the reconfiguration needed was local to the monitoring station only (i.e., switch from a passive, listening-only mode, to an active mode to receive and transmit messages). The network was able to detect the presence and the capability of the new node and to use it as soon as it became available. This is visible in Figure 17 with vehicle ecoSUBm5 157 that started to receive range measurements from node ID 1 as soon as it was deployed and in communication

range. Note also that, thanks to the usage of the CSMA protocol, the addition of the new node did not impact on the positional update rate of the vehicle. This is in contrast with the majority of the acoustic communication networks that are based on strict time divided transmissions and for which the addition of a node or vehicle requires the reconfiguration of every other node, reducing the network throughput to accommodate for the new addition.

Note also the presence of a few evident outliers coming from node 11 and node 23 (Figure 17) which were correctly filtered as described in Section 2.2. The difference between the estimated path followed by the vehicle (Figure 16, red line) and the reference path of the mission (Figure 16, black line) is due to the fact that the lawn-mower is implemented as a sequence of "go to waypoint" behaviours, as described in Section 2.3. The line-of-sight guidance law drives the vehicle directly to the destination waypoint (no heading constraint) rather than to the line joining two consecutive waypoints, resulting in the cross-track errors visible in Figure 16. Performances can be easily improved replacing the "go to waypoint" behaviour with a "track-following" behaviour (McPhail and Pebody, 1998) as the main building block for the lawn-mower.

For this mission, the surfacing error at the end of the mission was 25 m, corresponding approximately to 0.27% of the total distance traveled (approximately 9.5 km). For comparison, the reconstructed DR error was instead 675 m, corresponding to the 7.15% of the distance traveled.

5. Discussions and lessons learnt

The obtained results show that the proposed navigation system is able to estimate the position of the vehicles with an accuracy that is sufficient to successfully complete complex missions. Table 3 shows that the compared navigation systems exhibit consistent performance (i.e., of similar order of magnitude) in relation to the mission length. The only exception is represented by the fourth run of vehicle 154 during mission M3, where the dead-reckoner performed slightly better than other missions, possibly due to milder environmental conditions. Moreover, runs of ecoSUBm5 154 during mission M3 are also relatively short (about 10 minutes/500 metres long) and this limits their statistical importance. When longer missions are considered (distance traveled $\geq$1000 m), it is possible to observe that the surfacing error of the dead-reckoner can be reduced by 69% and up to 96% when using networked cooperative navigation (see last column of Table 3). This corresponds to a substantial average reduction of the surfacing error from 5.58% to 0.68% of the distance traveled. It is also worth noticing that the error reduction becomes more evident as the mission length increases (compare the data of ecoSUBm5 157 in Table 3, for instance). This is a clear indication that the drift of the error affecting the dead-reckoned navigation can be effectively bounded by the proposed solution. As expected, the overall performance depends on the number of anchor points (i.e., vehicles at the surface with GPS access) that are visible.

Unfortunately, vehicle and experimental limitations made it difficult to have a reliable ground truth to thoroughly evaluate the navigation performance. For underwater experiments this is a known issue (Bernardi et al., 2021). For the considered scenario, where GPS is not available, a possible alternative could use an independent acoustic positioning system. This would need to be fitted on each underwater vehicle, which, given the small size of the ecoSUBs would require substantial redesign and costs. Another alternative, at least for short-range underwater navigation, is the usage of a DVL to limit the growth of integration errors. For the ecoSUBs however, this is particularly challenging due to their size and a suitable DVL was not available for on-board usage. Despite the limitations of the experimental conditions (e.g., hardware problems impacting vehicle performance) the quality of the results given by the proposed navigation solution is not weakened and demonstrated that the presence of a network of cooperating vehicles/nodes is able to overcome the limitations of single individual platforms. In the presented experiment, a low-cost vehicle with limited localization ability was able to cross a high-current channel multiple times, covering a distance of about 9.5 km, with an end-of-mission error of 25 m. This is typically sufficient to perform monitoring missions (Ferri et al., 2017; Ferri et al., 2018), plume tracking or contour following (Jayasiri et al., 2016).

The experimental results have also highlighted the importance of having a thorough characterization of the environment to support post-mission data analysis. The availability of sound speed profiles in the mission area would make it possible to better characterize acoustic performance, and direct measurement of water currents would make it easier to analyse navigation errors. As discussed in (Bernardi et al., 2021), the complexity of at-sea experiments in terms of logistics, costs, and resources make the availability of environmental data difficult to obtain. Although the system was designed to support a full adaptive and cross-functional layering for navigation, localization, autonomy and communications, experimental constraints made possible to test the communication and localization services. The proposed networked system was able to detect communication and localization gaps and to forward the information onto the autonomy system. However, during the experiments, no action was implemented at the autonomy level to react in real time to it. In this case, once the information is available in the system, the implementation of adaptive behaviours that optimize mission performance can be done for example as proposed in (Caiti et al., 2013; Munafò et al., 2015), or in (Budd et al., 2022), where the network discussed in this work has been coupled with a planning strategy for data retrieval.

6. Conclusions

This paper described the design and implementation of an *ad hoc* acoustic sensor network of micro-AUVs with the final objective of enabling operation of a fleet of small, low-cost underwater vehicles in harsh, high-current, and tidal environments. The network leverage cross-functional layers to move the majority of the communication processing from the physical level to the network or application layers, and in this way making available autonomy, navigational and communication services that can be exploited to increase the system flexibility. Each node in the network is implemented on a AUV, making it possible for the network to adapt as needed as the environment change. The system was deployed in the Zadar Channel, Croatia, in October 2019 using pre-production prototype ecoSUB AUV units. A set of increasingly complex experiments were performed to validate the concept. The most complex network was composed of seven nodes, four surface nodes and three underwater vehicles. Results show how the network-enabled localization system was able to substantially increase the navigation performance, limiting the navigation error.

A behaviour-based architecture has been used to maintain a desired network geometry. In this work, a station keep behaviour was used to limit the experimental complexity, but it is easy to see how the proposed approach can be generalized to include more complex behaviour where each node can distributively optimize a cost function that includes, for example, the quality of communications and localization, while the communication layers are used to infer metrics on the channel state, and maintain a topography of the locations of devices in the fleet. This work also shows how the exploitation of the presence of a network can represent a step change for the usage of low cost micro-AUVs with limited sensing capabilities. For example, during the experiments the agents were able to establish an *ad hoc* network and the network was mostly used to improve their navigation. More in general, the presence of embedded electronics on each node, and of communications makes it possible for the network to provide more services to cooperatively solve complex tasks through local computation and communications.

Acknowledgments

The initial development of the ecoSUB AUVs was funded by Innovate UK under the project "Launch & Recovery of Multiple AUVs from an USV," project reference 102302. Development of *ad hoc* network was funded by Innovate UK under the project "LCAT: Low Cost AUV Technology: development of smart networks and AI Based Navigation for dynamic underwater environments," project reference 104058. Development of the V3 Nano modem was funded by EPSRC under the project "USMART - smart dust for large scale underwater wireless sensing," project reference EP/P017975/1. The authors would like to thank Terry Sloane, Iain Vincent and Alex Downer

from Planet Ocean Ltd/ecoSUB Robotics Ltd, the Newcastle University LCAT team and everyone that participated in the Innovate UK funded project LCAT for their continued support and the fruitful discussions. Finally the authors would like to thank the organising committee of Breaking the Surface (BtS) 2019 for hosting the project team.

ORCID

Davide Fenucci https://orcid.org/0000-0002-0338-3428
Jeremy Sitbon https://orcid.org/0000-0001-7594-4397
Jeffrey Neasham https://orcid.org/0000-0001-6059-9826
Alexander B. Phillips https://orcid.org/0000-0003-3234-8506
Andrea Munafò https://orcid.org/0000-0003-2284-0011

References

Bahr, A., Leonard, J. J., and Fallon, M. F. (2009a). Cooperative localization for autonomous underwater vehicles. *The International Journal of Robotics Research*, 28(6):714–728.

Bahr, A., Walter, M. R., and Leonard, J. J. (2009b). Consistent cooperative localization. In *2009 IEEE International Conference on Robotics and Automation*, pages 3415–3422.

Basagni, S., Petrioli, C., Petroccia, R., and Stojanovic, M. (2012). Optimized packet size selection in underwater wireless sensor network communications. *IEEE Journal of Oceanic Engineering*, 37(3):321–337.

Bernardi, M., Hosking, B., Petrioli, C., Bett, B. J., Jones, D., Huvenne, V. A., Marlow, R., Furlong, M., McPhail, S., and Munafò, A. (2021). AURORA, a multisensor dataset for robotic ocean exploration. *The International Journal of Robotics Research*, 0(0):02783649221078612.

Bosch Sensortec (2020). *BNO055 data sheet - Intelligent 9-axes absolute orientation sensor*. Bosch. Available at https://www.bosch-sensortec.com/media/boschsensortec/downloads/datasheets/bst-bno055-ds000.pdf.

Budd, M., Salavasidis, G., Kamarudzaman, I., Harris, C. A., Phillips, A. B., Duckworth, P., Hawes, N., and Lacerda, B. (2022). Probabilistic Planning for AUV Data Harvesting from Smart Underwater Sensor Networks. In *Submitted to the 2022 IEEE/RSJ International Conference on Intelligent Robots and Systems (IROS 2022)*.

Caiti, A., Calabrò, V., Munafò, A., Dini, G., and Lo Duca, A. (2013). Mobile Underwater Sensor Networks for Protection and Security: Field Experience at the UAN11 Experiment. *Journal of Field Robotics*, 30(2):237–253.

Dol, H. S., Casari, P., van der Zwan, T., and Otnes, R. (2017). Software-Defined Underwater Acoustic Modems: Historical Review and the NILUS Approach. *IEEE Journal of Oceanic Engineering*, 42(3):722–737.

Eickstedt, D. P. and Sideleau, S. R. (2010). The Backseat Control Architecture for Autonomous Robotic Vehicles: A Case Study with the Iver2 AUV. *Marine Technology Society Journal*, 44(4):42–54.

Fallon, M. F., Papadopoulos, G., and Leonard, J. J. (2010). A measurement distribution framework for cooperative navigation using multiple auvs. In *2010 IEEE International Conference on Robotics and Automation*, pages 4256–4263.

Fenucci, D. and Munafò, A. (2020). Experimental evaluation of outliers filtering techniques in networked acoustic localisation systems. In *Proceedings of 21th IFAC World Congress*, volume 53, pages 14582–14588.

Fenucci, D., Munafo, A., Phillips, A. B., Neasham, J., Gold, N., Sitbon, J., Vincent, I., and Sloane, T. (2018). Development of smart networks for navigation in dynamic underwater environments. In *2018 IEEE/OES Autonomous Underwater Vehicle Workshop (AUV)*, pages 1–6. IEEE.

Ferri, G., Munafò, A., and LePage, K. D. (2018). An autonomous underwater vehicle data-driven control strategy for target tracking. *IEEE Journal of Oceanic Engineering*, 43(2):323–343.

Ferri, G., Munafò, A., Tesei, A., Braca, P., Meyer, F., Pelekanakis, K., Petroccia, R., Alves, J., Strode, C., and LePage, K. (2017). Cooperative robotic networks for underwater surveillance: an overview. *IET Radar, Sonar & Navigation*, 11(12):1740–1761.

Ferri, G., Stinco, P., De Magistris, G., Tesei, A., and LePage, K. D. (2020). Cooperative Autonomy and Data Fusion for Underwater Surveillance With Networked AUVs. In *2020 IEEE International Conference on Robotics and Automation (ICRA)*, pages 871–877.

Hamilton, A., Holdcroft, S., Fenucci, D., Mitchell, P., Morozs, N., Munafò, A., and Sitbon, J. (2020). Adaptable underwater networks: The relation between autonomy and communications. *Remote Sensing*, 12(20).

Huang, X., Pascal, R. W., Chamberlain, K., Banks, C. J., Mowlem, M., and Morgan, H. (2011). A miniature, high precision conductivity and temperature sensor system for ocean monitoring. *IEEE Sensors Journal*, 11(12):3246–3252.

Intel (2021). *Intel Edison Development Platform*. Intel. Available at https://www.intel.com/content/dam/support/us/en/documents/edison/sb/edison_pb_331179002.pdf.

Jaffe, J., Franks, P., Roberts, P., Mirza, D., Schurgers, C., Kastner, R., and Bosh, A. (2017). A swarm of autonomous miniature underwater robot drifters for exploring submesoscale ocean dynamics. *Nature Communications*, 8.

Jayasiri, A., Gosine, R. G., Mann, G. K. I., and McGuire, P. (2016). AUV-Based Plume Tracking: A Simulation Study. *Journal of Control Science and Engineering*.

Jiang, S. (2018). State-of-the-Art Medium Access Control (MAC) Protocols for Underwater Acoustic Networks: A Survey Based on a MAC Reference Model. *IEEE Communications Surveys & Tutorials*, 20(1):96–131.

Jones, D. O., Gates, A. R., Huvenne, V. A., Phillips, A. B., and Bett, B. J. (2019). Autonomous marine environmental monitoring: Application in decommissioned oil fields. *Science of the total environment*.

Li, Y., Wang, Y., Yu, W., and Guan, X. (2019). Multiple autonomous underwater vehicle cooperative localization in anchor-free environments. *IEEE Journal of Oceanic Engineering*, 44(4):895–911.

Śliwka, J., Petroccia, R., Munafò, A., and Djapic, V. (2017). Experimental evaluation of Net-LBL: An acoustic network-based navigation system. In *OCEANS 2017 - Aberdeen*, pages 1–9.

Lowes, G. J., Neasham, J. A., Burnett, R., and Tsimenidis, C. C. (2019). Low energy, passive acoustic sensing for wireless underwater monitoring networks. In *OCEANS 2019 MTS/IEEE SEATTLE*, pages 1–9. IEEE.

Maczka, D. K., Gadre, A. S., and Stilwell, D. J. (2007). Implementation of a cooperative navigation algorithm on a platoon of autonomous underwater vehicles. In *OCEANS 2007*, pages 1–6.

McPhail, S. and Pebody, M. (1998). Navigation and control of an autonomous underwater vehicle using a distributed, networked, control architecture. *Oceanographic Literature Review*, 45(7):1240.

Munafò, A., Śliwka, J., and Alves, J. (2015). Dynamic placement of a constellation of surface buoys for enhanced underwater positioning. In *OCEANS 2015 - Genova*, pages 1–6.

Munafò, A. and Ferri, G. (2017). An acoustic network navigation system. *Journal of Field Robotics*, 34(7):1332–1351.

Munafò, A., Śliwka, J., and Petroccia, R. (2018). Localisation using undersea wireless networks. In *2018 OCEANS - MTS/IEEE Kobe Techno-Oceans (OTO)*, pages 1–7.

Myring, D. (1976). A theoretical study of body drag in subcritical axisymmetric flow. *The Aeronautical Quarterly*, 27(3):186–194.

Neasham, J. A., Goodfellow, G., and Sharphouse, R. (2015). Development of the "Seatrac" miniature acoustic modem and USBL positioning units for subsea robotics and diver applications. In *OCEANS 2015 - Genova*, pages 1–8.

Newcastle University and Heriott Watt and University of York (2021). USMART: Smart dust for large scale underwater wireless sensing. https://research.ncl.ac.uk/usmart/. Accessed: 2021-07-02.

Orlic, M., Gacic, M., and Violette, P. E. L. (1992). The currents and circulation of the Adriatic Sea. *OCEANOLOGICA ACTA*, 15(2).

Paull, L., Saeedi, S., Seto, M., and Li, H. (2014a). AUV navigation and localization: A review. *IEEE Journal of Oceanic Engineering*, 39(1):131–149.

Paull, L., Seto, M., and Leonard, J. J. (2014b). Decentralized cooperative trajectory estimation for autonomous underwater vehicles. In *2014 IEEE/RSJ International Conference on Intelligent Robots and Systems*, pages 184–191.

Peterson, K. M. (2003). Satellite communications. In Meyers, R. A., editor, *Encyclopedia of Physical Science and Technology (Third Edition)*, pages 413–438. Academic Press, New York, third edition edition.

Petrioli, C., Petroccia, R., and Stojanovic, M. (2008). A comparative performance evaluation of MAC protocols for underwater sensor networks. In *OCEANS 2008*, pages 1–10.

Phillips, A. B., Gold, N., Linton, N., Harris, C. A., Richards, E., Templeton, R., Thuné, S., Sitbon, J., Muller, M., Vincent, I., et al. (2017). Agile design of low-cost autonomous underwater vehicles. In *OCEANS 2017-Aberdeen*, pages 1–7. IEEE.

Phillips, A. B., Salavasidis, G., Kingsland, M., Harris, C., Pebody, M., Templeton, D. R. R., McPhail, S., Prampart, T., Wood, T., Taylor, R., and Jones, T. (2018). Autonomous surface/subsurface survey system field trials. In *2018 IEEE/OES Autonomous Underwater Vehicle Workshop (AUV)*, pages 1–6.

Quigley, M., Conley, K., Gerkey, B., Faust, J., Foote, T., Leibs, J., Wheeler, R., and Ng, A. Y. (2009). ROS: an open-source robot operating system. In *ICRA workshop on open source software*, volume 3, page 5. Kobe, Japan.

Quraishi, A., Bahr, A., Schill, F., and Martinoli, A. (2019). Easily deployable underwater acoustic navigation system for multivehicle environmental sampling applications. In *2019 International Conference on Robotics and Automation (ICRA)*, pages 3464–3470.

Roumeliotis, S. and Bekey, G. (2002). Distributed multirobot localization. *IEEE Transactions on Robotics and Automation*, 18(5):781–795.

Ruckdeschel, P., Spangl, B., and Pupashenko, D. (2014). Robust Kalman tracking and smoothing with propagating and nonpropagating outliers. *Statistical Papers*, 55(1):93–123.

Schill, F., Bahr, A., and Martinoli, A. (2018). Vertex: A new distributed underwater robotic platform for environmental monitoring. In *Distributed Autonomous Robotic Systems*, pages 679–693. Springer.

SeeByte, ltd. (2021). *Neptune Technical Whitepaper*. SeeByte, ltd. Available at https://www.seebyte.com/media/1427/neptune-technical-whitepaper.pdf.

Sherlock, B., Morozs, N., Neasham, J., and Mitchell, P. (2022). Ultra-low-cost and ultra-low-power, miniature acoustic modems using multipath tolerant spread-spectrum techniques. *Electronics*, 11(9):1446.

Simon, D. (2006). *Optimal state estimation: Kalman, H infinity, and nonlinear approaches*, chapter 5, pages 139–141. John Wiley & Sons.

SkyTraq Technology, Inc. (2011). *Venus638FLPx GPS Receiver Data Sheet*. SkyTraq Technology, Inc. Available at http://cdn.sparkfun.com/datasheets/Sensors/GPS/Venus638FLPx.pdf.

Song, A., Stojanovic, M., and Chitre, M. (2019). Editorial underwater acoustic communications: Where we stand and what is next? *IEEE Journal of Oceanic Engineering*, 44(1):1–6.

University of Zagreb (2021). Breaking the Surface - BTS. http://bts.fer.hr/. Accessed: 2021-07-02.

Vermeij, A. and Munafò, A. (2015). A robust, opportunistic clock synchronization algorithm for ad hoc underwater acoustic networks. *IEEE Journal of Oceanic Engineering*, 40(4):841–852.

Webster, S. E., Eustice, R. M., Singh, H., and Whitcomb, L. L. (2012). Advances in single-beacon one-way-travel-time acoustic navigation for underwater vehicles. *The International Journal of Robotics Research*, 31(8):935–950.

Zorzi, M. and Chockalingam, A. (2003). Wireless communications. In Meyers, R. A., editor, *Encyclopedia of Physical Science and Technology (Third Edition)*, pages 851–874. Academic Press, New York, third edition edition.

How to cite this article: Fenucci, D., Sitbon, J., Neasham, J., Phillips, A. B., & Munafò, A. (2022). *Ad hoc* acoustic network aided localization for micro-AUVs. *Field Robotics, 2*, 1888–1919.